

REPUBLIQUE ALGERIENNE DEMOCRATIQUE ET POPULAIRE
MINISTERE DE L'ENSEIGNEMENT SUPERIEUR ET DE LA RECHERCHE SCIENTIFIQUE
UNIVERSITE MOHAMED BOUDIAF - M'SILA

FACULTE DES SCIENCES
DEPARTEMENT PHYSIQUE
N° : PH/MAT/01/2022



DOMAINE : Sciences de la matière
FILIERE : Physique
OPTION : Physique des Matériaux

Mémoire présenté pour l'obtention
Du diplôme de Master Académique

Par: Refeida MEFTAH

Intitulé

**Theoretical investigation of structural, electronic and
magnetic properties of Heusler alloys**

Soutenu le / /2022 devant le jury composé de:

Berarma Khadidja	Université de Msila	Président
Saad Essaoud Saber	Université de Msila	Rapporteur
Ketfi Mohamed El-amine	Université de Msila	Examineur

Année universitaire : 2021/2022

شكر وعرفان

لله الحمد قيم السماوات والأرض ومن فيهن وله الحمد نور السماوات والأرض

ومن فيهن ..

لله الشكر أن أنعم علينا بنعم العقل والدين .. ووفقني لهذا الإنجاز المتواضع

وألهمني الصبر على العقبات ..

للتجارات أناس يقدرّون معناه.. وللإبداع أناس يحصدونه..

وعملا بقوله صلى الله عليه وآله وسلم " ..ومن صنع إليكم معروفا فكافئوه،

فإن لم تجدوا ما تكافئونه فادعوا له حتى تروا أنكم قد كافأتموه" رواه أبو داود

أتقدم بالشكر لأستاذي الكريم "ساعد السعود صابر" وأقدر جهوده المضنية

وتوجيهاته الثمينة ودعمه الامحدود .. فهو جدير بالثناء والشكر وله مني كل

التقدير..

جزاه الله خيرا عن كل حرف وجعله في ميزان حسناته ونفع به الأمة..

وأتوجه بجزيل الشكر إلى اللجنة، الأستاذة برارمة خديجة لتفضلها برئاسة

المناقشة والأستاذ كتفي محمد اللأمين لقبوله تقييم هذا العمل..

الاهداء

إلى من رباني و أنارا بالدعوات دربي ..

والدي الكريمين أدامهما الله ..

إلى الأحبة هناء هديل مؤمن سيف شهاب والوافد

الجديد رسيم ..

إلى غالياتي ورفيقات الشدة رميلة ابتسام وبسمة ..

إلى كل من علمني حرفا أو أفادني بعلم أو أعانني

بالنصيحة ..

أهدي عملي المتواضع..

Table of Contents

General introduction	1
----------------------	---

Chapter 1 : THEORETICAL STUDY OF A MANY-PARTICLES SYSTEM

1- The Schrödinger equation	4
2- Born-Oppenheimer approximation	5
3- Hartree and Hartree-Fock approximations (HF)	6
4- Density Functional Theory (DFT)	7
4-1 Formalism of density functional theory (DFT)	9
I- The theorems of Hohenburg and Kohn	9
A-1) First theorem	9
A-2) Second theorem	10
II- The Kohn - Sham equation	10
B-1) Solution of the Kohn - Sham equation	12
5- The different types of approximations of the <i>Excρ</i>	15
5-1 Local density approximation (LSDA)	15
5-2 The generalized gradient approximation GGA	16
6- Full-potential linearized augmented plane-wave method (FP-LAPW)	16
6-1 The plane wave method (APW)	16
6-2 The linearized augmented plane wave method (LAPW)	17
7- WIEN2K simulation code	19
8- References	22

Chapter 2: DFT-BASED SIMULATION ON SOME HEUSLER ALLOYS PROPERTIES

1- Heusler alloys family	26
2- Results and discussion	27
2-1 Computational details	27
2-2 Convergence tests	28
2-3 Structural properties	31
2-4 Electronic properties	34
2-4-1 Band structure	34
2-4-2 Electronic density of states	38
2-5 Magnetic properties	46
2-5-1 Origin of magnetism in materials	46
2-5-1-a Electron level	46
2-5-1-b Atomic level	47
2-5-1-c Material level	47
2-5-2 Basic types of magnetization	49
2-5-3 Magnetic properties of the Sc_2ZrX ($\text{X} = \text{P, As, Ge}$) compounds	50
3- References	52
 General conclusion	 55

List of Figures

Figure	I	1	Self-consistent calculation.	14
Figure	I	2	Diagram of the distribution of the elementary cell in atomic spheres and in interstitial region.	16
Figure	I	3	Programs incorporated in Wien2k code	21
Figure	II	1	Cubic crystal structure of X_2YZ full-Heusler alloys in $L2_1$ -type and X_a -type phases.	27
Figure	II	2	Convergence test of the total energy according to $R_{MTK_{max}}$.	29
Figure	II	3	Convergence test of the total energy according to k- points.	30
Figure	II	4	Total Energy-Volume Curves Sc_2ZrX ($X = P, As$ and Ge) in both $L2_1$ and X_a structure types calculated using GGA approximation.	33
Figure	II	5	Band structure of the Sc_2ZrAs compound obtained by GGA and mBJ Approximations.	35
Figure	II	6	The band structure of the Sc_2ZrP compound obtained by GGA and mBJ approximations.	36
Figure	II	7	The band structure of the Sc_2ZrGe compound obtained by GGA and mBJ approximations.	37
Figure	II	8	Total (TDOS) and partial (PDOS) density of states of the Sc_2ZrAs compound calculated with GGA approximation.	40
Figure	II	9	Total (TDOS) and partial (PDOS) density of states of the Sc_2ZrAs compound calculated with mBJ approximation.	41

Figure	II	10	Total (TDOS) and partial (PDOS) density of states of the Sc₂ZrP compound calculated with GGA approximation.	42
Figure	II	11	Total (TDOS) and partial (PDOS) density of states of the Sc₂ZrP compound calculated with mBJ approximation.	43
Figure	II	12	Total (TDOS) and partial (PDOS) density of states of the Sc₂ZrGe compound calculated with GGA approximation.	44
Figure	II	13	Total (TDOS) and partial (PDOS) density of states of the Sc₂ZrGe compound calculated with mBJ approximation.	45
Figure	II	14	Origin of magnetism at the electronic level.	46
Figure	II	15	Origin of magnetism at the atomic level.	47
Figure	II	16	Different cases of the exchange interaction between atoms.	48

List of Tables

Table	I	1	Comparison between the two methods, Hartree-Fock and the Density Functional Theory (DFT).	8
Table	II	1	Structural parameters of the Sc_2ZrX ($\text{X} = \text{P}, \text{As}, \text{Ge}$) compounds calculated using GGA approximation in both L2_1 and X_a structural phases.	32
Table	II	2	Types of magnetization.	49
Table	II	3	Total and partial magnetic moment of the Sc_2ZrX ($\text{X} = \text{P}, \text{As}, \text{Ge}$) Compounds.	51

Introduction

Introduction

Heusler alloys have gotten a great experimental and theoretical attention in the latest decade due to their characteristics, since they are theoretically assumed as half metals at room temperature (RT) [1]. These Alloys have a high Curie temperature above RT [2,3], and intermetallic controllability for spin of states at the Fermi level [4].

Due to their physical properties, Heusler compounds have the advantage of emerging as basic materials in many research fields such as superconductivity, magnetism, thermoelectric devices [4–9],etc. Therefore, research has focused on this family of materials and their characteristics, notably those relevant to the half-metallic property necessary in a wide range of technology domains. Furthermore, the magnetic characteristics of these materials have attracted the interest of many researchers, as understanding the origins of magnetism in these materials is an important part of condensed matter physics study. For this reason we have been interested in studying Sc_2ZrX ($\text{X} = \text{P}, \text{As}, \text{Ge}$) Heusler alloys despite that there are few studies on these compounds in hoping that our work adds more fruitful information and represents a trusted and useful source about the properties of these compounds.

The aforementioned objectives were achieved theoretically, as first-principles calculations based on density functional theory considerably aided us in studying and comprehending the structural, electronic, and magnetic behavior of these compounds.

This work is divided into two chapters: in the first, we reviewed the foundations of density functional theory (DFT), the Kohn-Sham equations, and the approximations that allow us to estimate the potential of exchange-correlation, namely the generalized gradient GGA and modified Becke-Johnson approximations (mBJ). The obtained results are presented in the second chapter, where we used Wien2k code to compute structural parameters of all three Sc_2ZrP , Sc_2ZrAs , and Sc_2ZrGe compounds, such as lattice parameter, bulk modulus, and cohesive energy. We also investigated the electronic behavior by determining the band structure, total density of states (DOS), and partial density of states (PDOS), then investigating the magnetic behavior. Finally, we finished our work by a general conclusion.

References

- [1] X. Wang, Z. Cheng, G. Liu, Largest magnetic moments in the half-Heusler alloys XCrZ (X= Li, K, Rb, Cs; Z= S, Se, Te): A first-principles study, *Materials*. 10 (2017) 1078.
- [2] B.T. Miller, L. Hug, T. Helbling, Potential of Thermoelectrics for Waste Heat Recovery, (n.d.).
- [3] H.Y. Lee, J.K. Lee, Dissolution of Thermoelectric Materials Containing Te with Acidic Solutions, *Sep. Sci. Technol.* 50 (2015) 1665–1670.
- [4] K. Elphick, W. Frost, M. Samiepour, T. Kubota, K. Takanashi, H. Sukegawa, S. Mitani, A. Hirohata, Heusler alloys for spintronic devices: review on recent development and future perspectives, *Sci. Technol. Adv. Mater.* 22 (2021) 235–271.
<https://doi.org/10.1080/14686996.2020.1812364>.
- [5] S.B. Riffat, X. Ma, Thermoelectrics: a review of present and potential applications, *Appl. Therm. Eng.* 23 (2003) 913–935.
- [6] L.E. Bell, Cooling, heating, generating power, and recovering waste heat with thermoelectric systems, *Science*. 321 (2008) 1457–1461.
- [7] L. Huang, Q. Zhang, B. Yuan, X. Lai, X. Yan, Z. Ren, Recent progress in half-Heusler thermoelectric materials, *Mater. Res. Bull.* 76 (2016) 107–112.
- [8] W.G. Zeier, J. Schmitt, G. Hautier, U. Aydemir, Z.M. Gibbs, C. Felser, G.J. Snyder, Engineering half-Heusler thermoelectric materials using Zintl chemistry, *Nat. Rev. Mater.* 1 (2016) 1–10.
- [9] T. Zhu, C. Fu, H. Xie, Y. Liu, X. Zhao, High efficiency half-Heusler thermoelectric materials for energy harvesting, *Adv. Energy Mater.* 5 (2015) 1500588.

CHAPTER 1

CHAPTER 1:

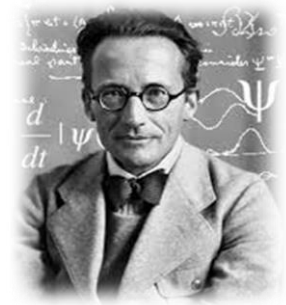
THEORETICAL STUDY OF MANY-PARTICLES SYSTEM

Table of Contents

1- The Schrödinger equation	4
2- Born-Oppenheimer approximation	5
3- Hartree and Hartree-Fock approximations (HF)	6
4- Density Functional Theory (DFT)	7
4-1 Formalism of Density Functional Theory (DFT)	9
I. The theorems of Hohenburg and Kohn	9
A-1) First theorem	9
A-2) Second theorem	10
II. The Kohn - Sham equation	10
B-1) Solution of the Kohn - Sham equation	12
5-The different types of approximations of the <i>Excp</i>	15
5-1 Local density approximation (LSDA)	15
5-2 The generalized gradient approximation GGA	16
6- Full-potential linearized augmented plane-wave method (FP-LAPW)	16
6-1 The plane wave method (APW)	16
6-2 The linearized augmented plane wave method (LAPW)	17
7- WIEN2K simulation code	19
8- References	22

1- The Schrödinger equation

In 1926, the physicist Erwin Schrödinger proposed a partial differential equation known as the Schrödinger equation in the framework of quantum theory [1]. The solution of this equation allows us to describe the instantaneous quantum state of a system through its wave function, which includes all the information about the system studied [2–4]. The Schrödinger equation has the following expression:



$$H\Psi(\vec{R}_I, \vec{r}_i) = E\Psi(\vec{R}_I, \vec{r}_i)$$

The two vectors \vec{R}_I and \vec{r}_i are the coordinates of the nucleus (I) and of the electron (i).

H: Hamiltonian operator related to the sum of the kinetic energy and the potential energy of the system.

E: Energy eigenvalue of the system.

Ψ : Wave function which depends on the coordinates of electrons and nuclei.

The Hamiltonian system - made up of nuclei and electrons - includes the kinetic energy of electrons and nuclei, as well as the potential energies (electron-electron, electron-nucleus, and nucleus-nucleus), therefore the expression of the total Hamiltonian of the system is written by the following expression:

$$H = T_e + T_N + V_{ee} + V_{e-N} + V_{N-N}$$

$$T_e = -\sum_i \frac{\hbar^2}{2m_i} \vec{\nabla}_i^2 \rightarrow \text{Electronic kinetic energy (} m_i \text{ the mass of electron } i \text{).}$$

$$T_n = -\sum_I \frac{\hbar^2}{2m_I} \vec{\nabla}_I^2 \rightarrow \text{Nuclei kinetic energy (} m_I \text{ the mass of the nucleus } I \text{).}$$

$$V_{N-N} = \sum_{I \neq J} \frac{Z_I Z_J e^2}{|R_I - R_J|} \rightarrow \text{The interaction part between the nuclei.}$$

$$V_{e-N} = \sum_{I,j} \frac{Z_I e^2}{|R_I - r_j|} \rightarrow \text{The nuclei-electrons interaction part.}$$

$$V_{e-e} = \sum_{i \neq j} \frac{e^2}{|r_i - r_j|} \rightarrow \text{The interaction part between the electrons.}$$

$|R_\alpha - R_\beta| \rightarrow$ The distance between the two nuclei α and β

$|r_i - R_\alpha| \rightarrow$ The distance between the nucleus α and the electron i

$|r_i - r_j| \rightarrow$ The distance between the two electrons i and j .

In practice, the Schrödinger equation is difficult to solve and the exact solution cannot be obtained, especially for systems containing large numbers of electrons and nuclei in motion and interaction between them, so simplifications and approximations must be used to obtain an approximate solution that is as close to the real solution as possible. The following are some of the most notable approximations and simplifications to the Schrödinger equation:

2- Born-Oppenheimer approximation

The Born-Oppenheimer approximation [5], developed in 1927 by physicists Max Born

and Robert Oppenheimer, allowed to separate the movement of nuclei from the movement of electrons.

Despite its movement, the nucleus remains very close to its equilibrium with respect to the electrons, which are very fast, and thus it is possible to ignore the nuclei's kinetic energy in regards to the electrons' kinetic energy and consider the nucleus-nucleus interaction energy as a

constant quantity ($V_{nn} = \text{Constant}$).

According to the Born-Oppenheimer approximation we can rewrite the total wave

function of the system $\Psi(\vec{R}_I^0, \vec{r}_i)$ in the form of a product of an electronic function $\Psi_e(\vec{R}_I^0, \vec{r}_i)$

and a nuclear function $\Psi_n(\vec{R}_I^0)$, thus, we can separate the motion of nuclei from that of

electrons. Then the wave function is written:

$$\Psi(\vec{R}_I^0, \vec{r}_i) = \Psi_n(\vec{R}_I^0) \Psi_e(\vec{R}_I^0, \vec{r}_i)$$

$$\begin{cases} [T_e + V_{ee} + V_{en}] \Psi_e(\vec{R}_I^0, \vec{r}_i) = E_e(\vec{R}_I^0) \Psi_e(\vec{R}_I^0, \vec{r}_i) \\ [T_n + V_{nn} + E_e(\vec{R}_I^0)] \Psi_n(\vec{R}_I^0) = E \Psi_n(\vec{R}_I^0) \end{cases}$$

Despite applying this simplification to the Schrödinger equation, the problem remains difficult and cannot be solved using current mathematical methods due to the extremely complicated electron-electron interaction, thus we used additional approximations.

3- Hartree and Hartree-Fock approximations (HF)

The Hartree-Fock approximation was proposed to modify and correct the shortcomings of the Hartree approximation. Hartree proposed in 1928 [6,7] that all electrons be treated as identical particles that move independently without interacting with other particles (independent particle approximation [8]). In this approximation, Hartree treats the interactions between electrons as particles carrying a charge without taking into account the spin state, i.e. the interactions that occur between them are Columbian repulsion interactions with neglecting both exchange and correlation terms. Furthermore, the wave function is not "anti-symmetric" since it does not take into consideration the Pauli exclusion principle [3,4].



Although the Hartree approximation does not take in account the electron spin and the Pauli exclusion principle, it simplifies the Schrödinger equation from studying a large number of electrons to studying a single electron, so that the total Hamiltonian H of electrons is the sum of the Hamiltonians h_i of each electron, while the total wave function of the electronic system represents by multiplication the individual wave functions of each electron [3,4]. Finally, the total energy of the electronic system is the sum of the energies of all electron. According to Hartree's approximation, the Hamiltonian equation for single electron can be written as follows:

$$H = \sum_i h_i$$

$$h_i = -\frac{\hbar^2}{2m_i} \Delta_i - \sum_I \frac{Z_I e^2}{|\vec{r}_i - \vec{R}_I^0|} + \frac{1}{2} \sum_j \frac{e^2}{|\vec{r}_i - \vec{r}_j|}$$

$$\Psi_e = \prod_i \Psi_i$$

$$E_e = \sum_i \varepsilon_i$$

In 1930, Fock [9] improved and modified Hartree's model by substituting the wave functions of the electron with a Slater determinant[10], allowing him to accommodate for the exchange effect that Hartree neglected. In this way, the interaction between electrons takes into account both the coulomb interaction and the exchange effect, and thus the previous functions have been replaced by anti-symmetric functions, and therefore, Fock introduced the term spin in its dealing with electronic interactions and replaced the wave function of the electronic system by a Slater determinant expressed by the formula:

$$\Psi_{HF}(\vec{r}_1, \vec{r}_2, \vec{r}_3, \dots, \vec{r}_N) = \frac{1}{\sqrt{N_e!}} \begin{bmatrix} \psi_1(\vec{r}_1) & \psi_1(\vec{r}_2) & \psi_1(\vec{r}_3) & \dots & \psi_1(\vec{r}_N) \\ \psi_2(\vec{r}_1) & \psi_2(\vec{r}_2) & \psi_2(\vec{r}_3) & \dots & \psi_2(\vec{r}_N) \\ \psi_3(\vec{r}_1) & \psi_3(\vec{r}_2) & \psi_3(\vec{r}_3) & \dots & \psi_3(\vec{r}_N) \\ \vdots & \vdots & \vdots & \ddots & \vdots \\ \psi_N(\vec{r}_1) & \psi_N(\vec{r}_2) & \psi_N(\vec{r}_3) & \dots & \psi_N(\vec{r}_N) \end{bmatrix}$$

Where $\frac{1}{\sqrt{N_e!}}$ is a normalization factor.

4- Density Functional Theory (DFT)

The aim behind Density Functional Theory (DFT) is to rewrite the Hamiltonian of the electron using electron density rather than wave functions. Researchers like Dirac [11], Slater [12], Hohenburg, and Kohn [13] have made significant contributions to this theory through their theoretical work.

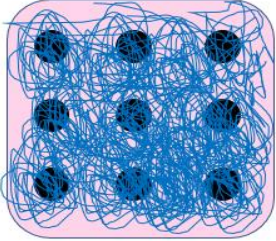
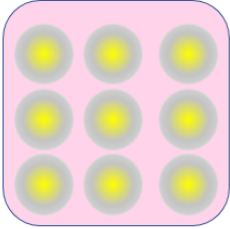
The DFT theory was first discovered in the works of Thomas and Fermi in 1927[13,4], where they created the main idea in expressing the total energy of an electronic system as a function of electron density by considering the electronic system as a homogeneous and regular gas of electrons where the continuous partitioning of the Brillouin zone (without taking into consideration electron correlations) was carried out by the two scientists Thomas and Fermi in order to achieve regions where the electron density is constant in each part. The following two formulas provide expressions for the density and kinetic energy of a homogeneous electronic gas:

$$\rho = \frac{1}{3\pi^2} E_f^{\frac{3}{2}} \left(\frac{2m_e}{h^2} \right)^{\frac{3}{2}}$$

$$E_c = \frac{3}{5} \left(\frac{h^2}{2m_e} \right) (3\pi^2)^{\frac{2}{3}} \rho^{\frac{5}{2}}$$

The following table presents a comparison between Hartree-Fock method and density functional theory and the characteristics of each method [3].

Table I. 1: Comparison between the two methods, Hartree-Fock and the Density Functional Theory (DFT) [16,17].

HF method	DFT
<div style="text-align: center;"> $\Psi(\mathbf{r})$  </div>	<div style="text-align: center;"> $E[\rho(\mathbf{r})]$  </div>
<ul style="list-style-type: none"> • Principle: Solving the Schrödinger equation by considering the wave functions as a variable basic. • Based on the mean field theory (MFT). • Calculates wave functions and eigenvalue energy to obtain ground state energy. • Depend on the large number of variables, which makes the equation very complicated and time consuming. • The wave functions obtained as solutions for the Schrödinger equation have no physical meaning. • Does not take into account the correlation terms. 	<ul style="list-style-type: none"> • Principle: Solving the Schrödinger equation by considering the electron density as a variable basic. • Based on the two Hohenburg – Sham theorems and shifting from the Schrödinger equation to the Kohn-Sham equations to find the solution. • Use electron density which has physical meaning. • Reduce the number of variables which makes the equation simpler and faster compared to the HF method. • Enable to treat the correlation terms.

4-1 Formalism of density functional theory (DFT)

The density functional theory (DFT) is based on describing the total energy of a system with many interacting electrons as a function of the electronic density, rather than its wave function, where the electronic density is expressed by the formula:

$$\rho(\vec{r}) = \sum_{i=1}^N |\Psi_i(\vec{r})|^2$$

The density functional theory (DFT) is based on two main theorems.

I. The theorems of Hohenburg and Kohn

The two theorems presented by Hohenburg and Kohn in 1964, are considered to be the basis of the density functional theory.



A-1) First theorem:

The total energy of an electronic system is a functional of the electron density for an external potential $V(\mathbf{r})$, so it is possible to know all the properties of the system when determining the electron density[3,18].



$$E[\rho] = F[\rho] + \int V(\vec{r})\rho(\vec{r})d\mathbf{r}^3$$

Where $F[\rho]$ is universal functional.

The external potential and the universal functional $F[\rho]$ are expressed in the form:

$$V_{ext}(\vec{r}_i) = - \sum_A \frac{Z_A}{r_{iA}}$$

$$F[\rho] = T[\rho] + U[\rho]$$

Where Z_A is the charge of the nucleus, r_{iA} is the distance between nucleus A and electron i .

A-2) Second theorem:

The second theory appears that to obtain the total energy of the ground state of the electronic system, it is enough to find the corresponding electron density which makes the density function at its minimum value.

$$E(\rho_0(\vec{r})) \leq E[\rho(\vec{r})]$$

$$E(\rho_0) = \text{Min} E(\rho) \lim_{\rho \rightarrow N} \langle \Psi | \hat{T} + \sum_i V_{ext} + V_{ee} | \Psi \rangle$$

We can get the corresponding electron density of the ground state, by applying the variational principle via the differential of total energy in terms of electron density:

$$\frac{dF[\rho(r)]}{d\rho(r)} + V(r) = 0$$

Therefore, if the electron density which minimizes the energy function is known, we can easily determine the wave function and the exact energy of the ground state.

II. The Kohn - Sham equation

One of the difficulties in studying a many-electrons system is the inability to express the kinetic energy and electron-electron interactions analytically in terms of electron density.



In 1965, scientists Kohn and Sham suggested the initial idea of replacing the real electronic system with a fictive system in which the behavior of the electron is independent, unrelated, and unaffected by the behavior of other electrons. It is only affected by the effective potential (Kohn-Sham potential), which involves both the external potential created by the nuclei's influence and the potential caused by the remaining particles effect on this electron[3,19,20].

The fictive system proposed by Kohn-Sham is characterized by:

- ✓ The Kohn-Sham orbits which are space wave functions of a single electron are solutions of the Schrödinger equation in this vacuum space.
- ✓ The fictive electronic system has the same electronic density as a real system.

- ✓ The kinetic energy of the fictive system is the kinetic energy of the electrons without the correlation effect and it is positive, while the kinetic energy in the real system “ T_R ” is the sum of the kinetic energy of the fictive system “ T_f ” and an additional term that expresses the effect of the correlation “ T_c ” on the kinetic energy of the electron [3] that is:

$$T_R = T_f + T_c$$

$$T_c = \langle \Psi | T | \Psi \rangle - \langle \varphi | T_s | \varphi \rangle$$

The V_{ee} interaction between electrons in the real system which is written in the following relation:

$$\langle \Psi | V_{ee} | \Psi \rangle = U_H + U_x + U_c$$

Where the terms represent:

U_H : The electron-electron coulomb interaction (Hartree potential)

U_x : The exchange energy between electrons of the same spin.

U_c : The correlation energy between the electrons.

The Kohn-Sham equation for an electronic system is given as a function of the kinetic energy of the electron: external potential energy, Hartree interaction and exchange-correlation energy as follows:

- ✓ The kinetic energy of an electron in a fictitious system:

$$T_s[\rho] = \left\langle \varphi_i \left| -\frac{\hbar^2}{2m} \Delta \right| \varphi_i \right\rangle = -\frac{\hbar^2}{2m} \sum_i \int \varphi_i \nabla^2 \varphi_i^* dr_i$$

- ✓ The external potential generated by the effect of nuclei (nucleus-electron interaction):

$$V_{NE}[\rho] = - \int \sum_{I,i} \frac{Z_I \rho(\vec{r})}{|\vec{R}_I^0 - \vec{r}|} dr$$

- ✓ The Hartree potential (electron-electron coulomb interaction)

$$U[\rho] = \frac{1}{2} \int \frac{\rho(\vec{r})\rho(\vec{r}')}{|\vec{r} - \vec{r}'|} dr dr'$$

- ✓ The exchange-correlation energy, which is the sum of the correlation and exchange terms, it does not have an exact mathematical expression, but it is estimated by approximations

$$E_{xc}[\rho] = E_x[\rho] + E_c[\rho]$$

And finally, the Kohn-Sham equation is written as follows [21–23]:

$$H_{KS}\varphi_i(\vec{r}) = [T_s[\rho] + V_{KS}(\vec{r})]\varphi_i(\vec{r}) = \varepsilon^{KS}\varphi_i(\vec{r})$$

$$V_{KS}(\vec{r}) = V_{ext}(\vec{r}) + V_H(\vec{r}) + V_{XC}(\vec{r})$$

$$E[\rho] = T_s[\rho] + V_{NE}[\rho] + U_H[\rho] + E_{xc}[\rho]$$

B-1) Solution of the Kohn - Sham equation

Solving the Kohn-Sham equation depends on two basic steps:

- The first step: define all the terms of the effective Kohn-Sham potential, i.e. the exchange-correlation potential E_{xc} must be determined because this term has no mathematical formula but it can be estimated by approximations.
- The second step: find the wave functions (Kohn-Sham orbits), which represent a solutions for the Kohn-Sham equation given by [3]:

$$\varphi_{KS}(\vec{r}) = \sum_j C_{ij} \varphi_j(\vec{r})$$

Where $\varphi_i(\vec{r})$ are the basic functions, and C_{ij} are the development coefficients.

$$\left\langle \sum_j C_{ij} H_{KS} \middle| \varphi_j \right\rangle = \left\langle \sum_j C_{ij} \varepsilon_{KS} \middle| \varphi_j \right\rangle$$

$$\left\langle \varphi_k \middle| \sum_j C_{ij} H_{KS} \middle| \varphi_j \right\rangle = \left\langle \varphi_k \middle| \sum_j C_{ij} \varepsilon_{KS} \middle| \varphi_j \right\rangle$$

$$\sum_j (\langle \varphi_k | H_{KS} | \varphi_j \rangle - \varepsilon_{KS} \langle \varphi_k | \varphi_j \rangle) C_{ij} = 0$$

It remains to determine the C_{ij} coefficients.

The Kohn-Sham equation is solved according to an iterative cycles illustrated by figure (1.I), where the process starts using an initial density ρ_{in} for the first iteration, this density is used to solve the Kohn-Sham equation, then, We use a superposition of the atomic densities and we compute the Kohn-Sham matrix, to solve the equations, then obtain the Kohn-Sham orbitals.

After this step, we calculate the new density ρ_{out} , to check the convergence condition (if the density or energy has changed a lot or not) and we mixed the two charge densities ρ_{out} and ρ_{in} as follow:

$$\rho_{in}^{i+1} = (1 - \alpha)\rho_{in}^i + \rho_{out}^i$$

Thus the iterative procedure can be repeated until the convergence condition is fulfilled.

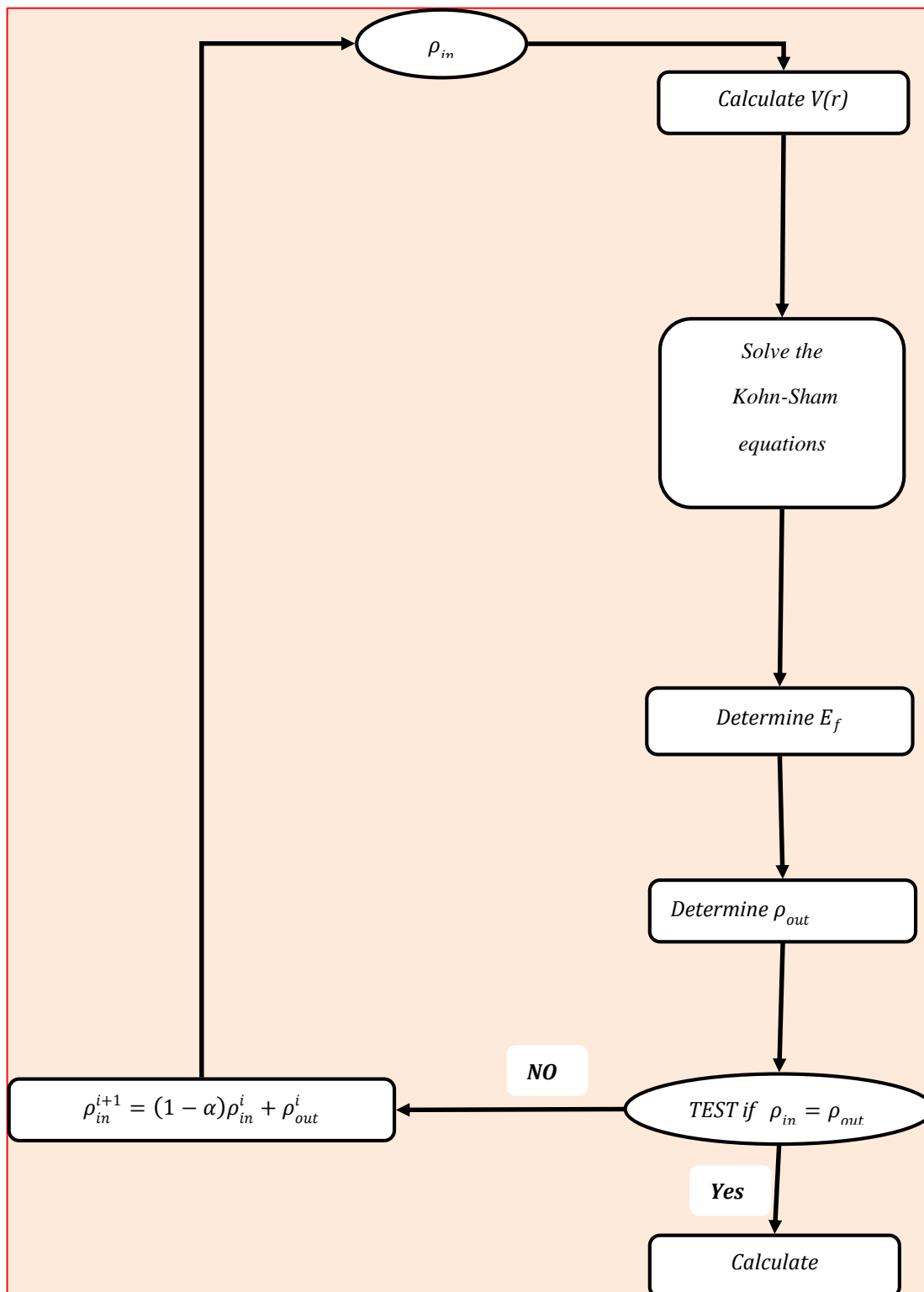


Figure I. 1: Self-consistent calculation.

5-The different types of approximations of the $E_{xc}[\rho]$

As the exchange-correlation potential between electrons has no analytical term, several scenarios have been used to obtain approximate values for this potential, the accuracy of the results obtained being mainly related to the mathematical formula of this potential[3].

5-1 Local density approximation (LSDA)

This model was first proposed by Kohn and Sham in 1964 [24] where the inhomogeneous electronic system is approximated by a local homogeneous electronic system after dividing the Brillouin region into small regions, and the expression energy exchange - correlation is given by the relation :

$$E_{XC}^{LSDA} = \int \rho(\vec{r}) E_{xc}[\rho(\vec{r})] d\vec{r}$$

$$V_{xc} = \frac{dE_{XC}^{LSDA}[\rho]}{d\rho} = \varepsilon_{XC}^{LSDA} + \rho(\vec{r}) \frac{d\varepsilon_{XC}^{LSDA}}{d\rho}$$

For each spin up or down magnetic order, the total electron density becomes the sum of the two electron densities

$$\rho(\vec{r}) = \rho_{\uparrow}(\vec{r}) + \rho_{\downarrow}(\vec{r})$$

The Kohn-Sham equation for the two spins in the form [3]:

$$\left\{ \begin{array}{l} \left(\frac{-\hbar^2}{2m} \nabla^2 + V_{eff}^{\uparrow}(\vec{r}) \right) \varphi_i(\vec{r}) = \varepsilon_{KS}^{\uparrow} \varphi_i(\vec{r}) \\ \left(\frac{-\hbar^2}{2m} \nabla^2 + V_{eff}^{\downarrow}(\vec{r}) \right) \varphi_i(\vec{r}) = \varepsilon_{KS}^{\downarrow} \varphi_i(\vec{r}) \end{array} \right.$$

The effective potential for the two spins is written as [3]:

$$\left\{ \begin{array}{l} V_{eff}^{\uparrow}(\vec{r}) = V_{ext} + V_{xc}^{\uparrow} = V_{ext} + \frac{d\varepsilon_{XC}^{LSDA}[\rho_{\uparrow}(\vec{r}), \rho_{\downarrow}(\vec{r})]}{d\rho_{\uparrow}(\vec{r})} \\ V_{eff}^{\downarrow}(\vec{r}) = V_{ext} + V_{xc}^{\downarrow} = V_{ext} + \frac{d\varepsilon_{XC}^{LSDA}[\rho_{\uparrow}(\vec{r}), \rho_{\downarrow}(\vec{r})]}{d\rho_{\downarrow}(\vec{r})} \end{array} \right.$$

5-2 The generalized gradient approximation GGA

The previous approximation considered the electron density to be uniformly distributed, making its density homogeneous, but this approximation produced results that were inconsistent with the experimental results on several times, so a new approximation was developed, in which the localized electron density was considered to be non-homogeneous and varied from place to place. Thus, the total energy of the electron system is proportional to both the electron density $\rho(\vec{r})$ and its gradient $\nabla\rho(\vec{r})$, as shown by the equation [25]:

$$E_{XC}^{GGA}[\rho(\vec{r})] = \int d^3\vec{r}\rho(\vec{r})\varepsilon_{XC}[\rho(\vec{r}),\nabla\rho(\vec{r})]$$

6- Full-potential linearized augmented plane-wave method (FP-LAPW)

After solving the exchange-correlation potential problem, the search for wave functions as solutions to the Kohn-Sham equation became necessary. After extensive research, certain approaches emerged, including the OPW method presented by Herring theory in 1940 [26], the LMTO method [27], and the FP-LAPW method, where these methods are dependent on the quality of the effective potential utilized.

6-1 The plane wave method (APW)

This method was carried out by the scientist Slater [10] who divided the crystal space into two parts based on the Muffin-Tin approximation [28] (see Figure I.2) by representing the atoms as non-overlapping spheres of radius R_0 in which the core electrons are located, and between these spheres, an interstitial region containing free electrons that are away from the nuclei of their atoms.

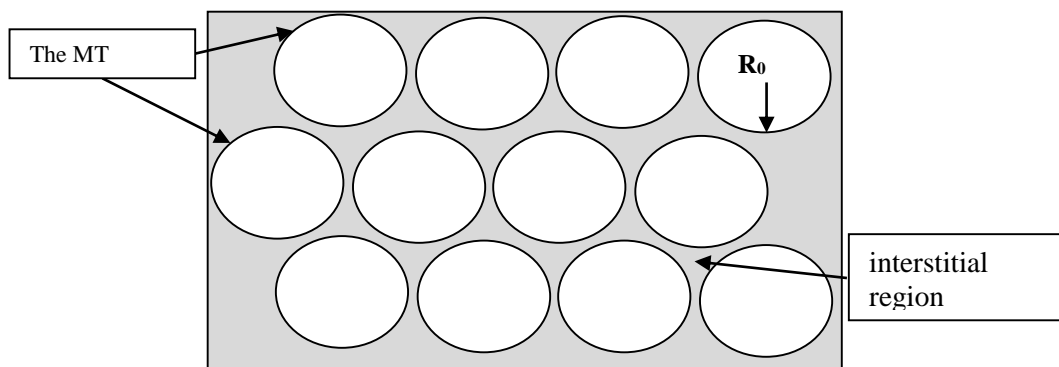


Figure I. 2: Diagram of the distribution of the elementary cell in atomic spheres and in interstitial region.

According to Slater's approximation [10], the core electrons located inside the sphere are subjected to the spherical potential, on the other hand, in the interstitial region the potential is constant [3]. So, the potential in the two regions is given in the form:

$$V(\vec{r}) = \begin{cases} V(r) & r \leq R_0 \\ 0 & r > R_0 \end{cases}$$

Also, the waves that describe the behavior of electrons inside MT spheres differ from those in the interstitial region, they are described by plane waves in the interstitial region, while inside spheres by functions radials multiplied by spherical harmonics[3]. The two different wave functions are given by the following expression:

$$\varphi(\vec{r}) = \begin{cases} \sum_{l=0}^{\infty} \sum_{-m}^m A_{lm} U_l(r) Y_{lm}(r) & r \leq R_0 \\ \frac{1}{\sqrt{\Omega}} \sum_{\vec{G}} C_{\vec{G}} e^{i(\vec{K}+\vec{G})\vec{r}} & r > R_0 \end{cases}$$

Where Ω : The cell volume

Y_{lm} : Spherical harmonics

A_{lm} : Development coefficients

U_l : The regular solution of the Schrödinger equation given by[29] :

$$\left(\frac{-d^2}{dr^2} + \frac{l(l+1)}{r^2} V(r) \right) r U_l = E_l U_l$$

Where E_l : An energy parameter.

6-2 The linearized augmented plane wave method (LAPW)

The downside of using the APW method is its slow process in calculations due to the common radial function U_l ; additionally, it is difficult to define the radial function for each value of energy E_l . So that, Anderson [30] made improvements to the APW method [31] by using the Taylor expansion to write the radial functions $U_l(r)$ in the following form:

$$U_l(r, E) = U_l(r, E_l) + (E_l - E) \left. \frac{dU_l(r, E)}{dE} \right|_{E=E_l} + O(E_l - E)^2$$

Where the term $O(E - E_l)^2$ represents the quadratic error.

After several simplifications, he has got the expression of potential inside and outside of Muffin-Tin balls as follows:

$$V(r) = \begin{cases} \sum_{lm}^m V_{lm}(r) Y_{lm} & r \leq R_0 \\ \sum_{lm}^m V_k(r) e^{ikr} & r > R_0 \end{cases}$$

As well as the wave functions inside the spheres in terms of radial functions and their derivatives. Where the wave functions are written as follows [32,33]:

$$\Phi_{\vec{K}+\vec{G}}(\vec{r}) = \begin{cases} \sum_{lm} (A_{lm} U_l(r) + B_{lm} \dot{U}_l(r)) Y_{lm}(r) & r \leq R_0 \\ \frac{1}{\sqrt{\Omega}} \sum_G C_G e^{i(\vec{K}+\vec{G})\vec{r}} & r > R_0 \end{cases}$$

Where:

\vec{K} : represents the wave vector.

\vec{G} : is the vector of the reciprocal lattice.

A_{lm} : are coefficients corresponding to the function U_l .

B_{lm} : are coefficients corresponding to the function U_l .

We can determine the coefficients A_{lm} and B_{lm} , for each wave vector, and for each atom by applying the conditions of continuity of the basic functions in the vicinity of the limit of the spheres. After some simplifications we find the coefficient formula A_{lm} and B_{lm} in the following forms:

$$A_{lm} = \frac{4\pi r_0^2 i^L}{\sqrt{\Omega}} Y_{lm}^*(K+G) a_l(K+G)$$

$$B_{lm} = \frac{4\pi r_0^2 i^L}{\sqrt{\Omega}} Y_{lm}^*(K+G) b_l(K+G)$$

7- WIEN2K simulation code

With the technological development, especially programming languages, researchers from the Institute of Materials Chemistry in Vienna were able to design the Wien2k program package [34], which is considered to be one of the most important programs used to study the properties of solid materials. This program consists of many subprograms written in Fortran language, the last of which are algorithms that translate the equations of the crystal system treated according to the density functional theory (DFT) which adopt the method of The full potential linearized augmented plane wave FP-LAPW as a way to compute algorithms to study the properties of compounds [3].

The most important subprograms and its role in the Wien2k code are shown in Figure I.3 which are organized as follows:[3]:

- ✓ **NN** : This subprogram calculates the distances between nearest neighbors up to a specified limit which therefore helps to determine the value of the radius of the atomic sphere.
- ✓ **SGROUP** : determines the space group of the compound.
- ✓ **SYMMETRY** : is a program that defines the symmetry number and space group symmetry operations of our structure.
- ✓ **LSTART** : calculates electron densities in free atoms and show how different orbitals will be treated in band structure calculations.
- ✓ **KGEN** : generates a mesh of K points in the irreducible part of the first Brillouin zone (B.Z). We specify the number of K points in the whole 1stB.Z.
- ✓ **DSTART** : produces an initial density for the SCF cycle (self-consistent cycle) by a superposition of atomic densities produced in the LSTART subprogram.

After the last subprogram ; we enter a loop of SFC calculations and therefore we shall reach five steps :

- ✓ **LAPW0 (POTENTIAL)** : uses the total electron density to calculate the coulomb and exchange potential (Hartree-Fock potential). In addition to that, it divides the space into a MT (muffin-tin) sphere and an interstitial region.
- ✓ **LAPW1 (BANDS)** : calculate eigenvalues and wave functions for valence electrons from solving the equation (III.1).
- ✓ **LAPW2 (RHO)** : calculate the valence electron densities obtained in the step LAPW0.
- ✓ **LCORE** : calculates eigenvalues and wave functions to obtain core electron densities.
- ✓ **MIXER** : calculate the new density by mixing.

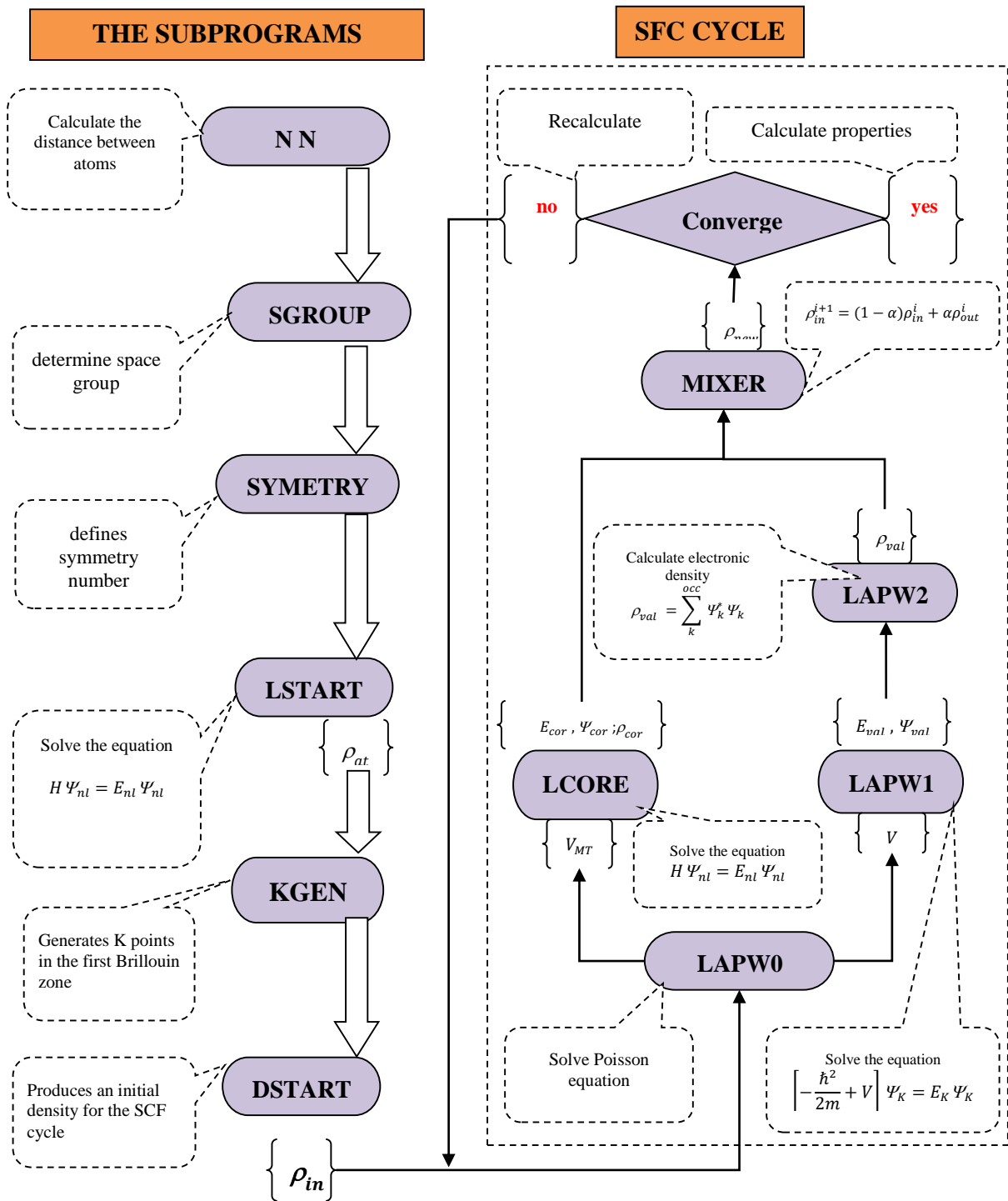


Figure I. 3 : Programs incorporated in Wien2k code [3].

8- References

- [1] E. SCHROEDINGER, Quantization as a Problem of Proper Values (Part I), *Ann. Phys.* (1926). <https://ci.nii.ac.jp/naid/10022177951/en/>.
- [2] S.S. Essaoud, M. Imadalou, D.E. Medjadi, Microscopic Study of Correlations in Finite Fermionic Systems by Breaking the Axial Symmetry, *Int J Mod. Theo Phys.* 5 (2016) 8–21.
- [3] S. Saad Essaoud, *Les composés à base de manganèse: investigation théorique des propriétés structurales électroniques et magnétiques*, 2020. <https://doi.org/10.13140/RG.2.2.30742.68169>.
- [4] S. Saad Essaoud, *Etude microscopique des corrélations dans les systèmes fermioniques finis en brisant la symétrie axiale*, 2013. <https://doi.org/10.13140/RG.2.2.19283.71203>.
- [5] M. Born, R. Oppenheimer, *Zur Quantentheorie der Molekeln*, *Ann. Phys.* 389 (1927) 457–484. <https://doi.org/10.1002/andp.19273892002>.
- [6] D.R. Hartree, The wave mechanics of an atom with a non-coulomb central field. Part II. Some results and discussion, in: *Math. Proc. Camb. Philos. Soc.*, Cambridge University Press, 1928: pp. 111–132.
- [7] D.R. Hartree, The wave mechanics of an atom with a non-coulomb central field. part iii. term values and intensities in series in optical spectra, in: *Math. Proc. Camb. Philos. Soc.*, Cambridge University Press, 1928: pp. 426–437.
- [8] G. Shadmon, I. Kelson, Multi-determinantal hartree-fock theory, *Nucl. Phys. A.* 241 (1975) 407–428. [https://doi.org/10.1016/0375-9474\(75\)90395-4](https://doi.org/10.1016/0375-9474(75)90395-4).
- [9] V. Fock, „Selfconsistent field “mit Austausch für Natrium, *Z. Für Phys.* 62 (1930) 795–805.
- [10] J.C. Slater, Damped Electron Waves in Crystals, *Phys. Rev.* 51 (1937) 840–846. <https://doi.org/10.1103/physrev.51.840>.
- [11] P.A.M. Dirac, Note on Exchange Phenomena in the Thomas Atom, *Math. Proc. Camb. Philos. Soc.* 26 (1930) 376–385. <https://doi.org/10.1017/S0305004100016108>.
- [12] J.C. Slater, A Simplification of the Hartree-Fock Method, *Phys. Rev.* 81 (1951) 385–390. <https://doi.org/10.1103/PhysRev.81.385>.
- [13] P. Hohenberg, W. Kohn, Inhomogeneous Electron Gas, *Phys. Rev.* 136 (1964) B864–B871. <https://doi.org/10.1103/physrev.136.b864>.

- [14] L.H. Thomas, The calculation of atomic fields, *Math. Proc. Camb. Philos. Soc.* 23 (1927) 542. <https://doi.org/10.1017/s0305004100011683>.
- [15] E. Fermi, Eine statistische Methode zur Bestimmung einiger Eigenschaften des Atoms und ihre Anwendung auf die Theorie des periodischen Systems der Elemente, *Z. Für Phys.* 48 (1928) 73–79.
- [16] للمركب CsVO₃ ل. مروة, دراسة الخواص الكهرو حرارية والترموديناميكية, Master Thesis, UNIVERSITE MOHAMED BOUDIAF-M'SILA, 2021.
- [17] آ. قريشي, دراسة نظرية للخواص البنوية, الإلكترونية والضوئية للمركبين AgMgF₃ k3MgF, Master Thesis, UNIVERSITE MOHAMED BOUDIAF-M'SILA, 2021.
- [18] R.M. Dreizler, E.K.U. Gross, *Density Functional Theory*, (1990). <https://doi.org/10.1007/978-3-642-86105-5>.
- [19] R. Stowasser, R. Hoffmann, What do the Kohn- Sham orbitals and eigenvalues mean?, *J. Am. Chem. Soc.* 121 (1999) 3414–3420.
- [20] A. Seidl, A. Görling, P. Vogl, J.A. Majewski, M. Levy, Generalized Kohn-Sham schemes and the band-gap problem, *Phys. Rev. B.* 53 (1996) 3764.
- [21] C. Fiolhais, F. Nogueira, M.A. Marques, *A primer in density functional theory*, Springer Science & Business Media, 2003.
- [22] F.M. Bickelhaupt, E.J. Baerends, Kohn-Sham density functional theory: predicting and understanding chemistry, *Rev. Comput. Chem.* 15 (2000) 1–86.
- [23] J.A. Pople, P.M. Gill, B.G. Johnson, Kohn—Sham density-functional theory within a finite basis set, *Chem. Phys. Lett.* 199 (1992) 557–560.
- [24] W. Kohn, L.J. Sham, Self-Consistent Equations Including Exchange and Correlation Effects, *Phys. Rev.* 140 (1965) A1133–A1138. <https://doi.org/10.1103/physrev.140.a1133>.
- [25] D.M. Ceperley, B.J. Alder, Ground State of the Electron Gas by a Stochastic Method, *Phys. Rev. Lett.* 45 (1980) 566–569. <https://doi.org/10.1103/physrevlett.45.566>.
- [26] C. Herring, A new method for calculating wave functions in crystals, *Phys. Rev.* 57 (1940) 1169.
- [27] H.L. Skriver, *The LMTO Method: Muffin-Tin Orbitals and Electronic Structure*, Springer-Verlag, Berlin Heidelberg, 1984. <https://doi.org/10.1007/978-3-642-81844-8>.
- [28] O.K. Andersen, T. Saha-Dasgupta, Muffin-tin orbitals of arbitrary order, *Phys. Rev. B.* 62 (2000) R16219.

- [29] D D Koelling and G O Arbman, Use of energy derivative of the radial solution in an augmented plane wave method: application to copper, *J. Phys. F Met. Phys.* 5 (1975) 2041.
- [30] O.K. Andersen, Linear methods in band theory, *Phys. Rev. B.* 12 (1975) 3060–3083. <https://doi.org/10.1103/physrevb.12.3060>.
- [31] M. Petersen, F. Wagner, L. Hufnagel, M. Scheffler, P. Blaha, K. Schwarz, Improving the efficiency of FP-LAPW calculations, *Comput. Phys. Commun.* 126 (2000) 294–309.
- [32] D.R. Hamann, Semiconductor Charge Densities with Hard-Core and Soft-Core Pseudopotentials, *Phys. Rev. Lett.* 42 (1979) 662–665. <https://doi.org/10.1103/physrevlett.42.662>.
- [33] M. Weinert, Solution of Poisson's equation: Beyond Ewald-type methods, *J. Math. Phys.* 22 (1981) 2433–2439. <https://doi.org/10.1063/1.524800>.
- [34] P. Blaha, K. Schwarz, G. Madsen, D. Kvasnicka, J. Luitz, *Wien2k*, (2001).

CHAPTER 2

CHAPTER 2:**DFT-BASED SIMULATION ON SOME HEUSLER ALLOYS PROPERTIES**

Contents

1- Heusler alloys family	26
2-Results and discussion	27
2-1 Computational details	27
2-2 Convergence tests	28
2-3 Structural properties	31
2-4 Electronic properties	34
2-4-1 Band structure	34
2-4-2 Electronic density of states	38
2-5 Magnetic properties	46
2-5-1 Origin of magnetism in materials	46
2-5-1-a Electron level	46
2-5-1-b Atomic level	47
2-5-1-c material level	47
2-5-2 Basic types of magnetization	49
2-5-3 Magnetic properties of the Sc₂ZrX (X = P, As, Ge) compounds	50
3-References	52

1- Heusler alloys family

Heusler alloys were discovered in 1903, when Heusler revealed that the addition of “*sp*” elements (Al, In, Sn, Sb, or Bi) transforms a Cu-Mn alloy into a ferromagnetic material despite the alloy containing no ferromagnetic elements [1]. After this discovery, research intensified in order to reveal the properties of numerous compounds belonging to this family, which were later classified according to the chemical formula and the positions of the atoms that make up them into four types:

- Half-Heusler Alloys (HHA) with \mathbf{XYZ} chemical formula (more details in reference [2]).
- Full-Heusler Alloys (FHA) with $\mathbf{X_2YZ}$ chemical formula (more details in reference[3]).
- Quaternary Heusler alloys (QHA) with $\mathbf{XX'YZ}$ chemical formula (more details in reference [4,5]).
- Half-Heusler Alloys (DHA) with $\mathbf{X_2YY'Z_2}$ chemical formula (more details in reference[6,7]).

In our work, we have studied three compounds belonging to the second group of Heusler compounds.

Ternary Heusler alloys have X_2YZ formula composed by three elements: X and Y are two transition metals while the Z is in the p-block, and in some cases X_2YZ Heusler alloys contain four atoms. According to the position occupied by these atoms, we distinguish two types of structures symbolized $L2_1$ -type ($\mathbf{Cu_2MnAl}$ structure, space group Fm-3m (225)) and X_α ($\mathbf{Hg_2CuTi}$ type) with space group F-43m (216) [3,8]. Each atom in the alloys can occupy one of the following four sites: A(0.0.0), B(1/4.1/4.1/4), C(1/2.1/2.1/2), and D (3/4.3/4.3/4). As it is also known that the physical properties of crystals depend directly on their structural properties, therefore any change in the arrangement of the atoms' position in all the two phases affects the properties of the compound as we will see later. In both types of structures, X and Z atoms take places A and D, while the difference between the two phases remains in the place that the atom Y will occupy. As shown in Figure II.1, we note that the Y atom takes place in C site in the X_α phase, while it occupied B site in the other ($L2_1$) phase [3,8].

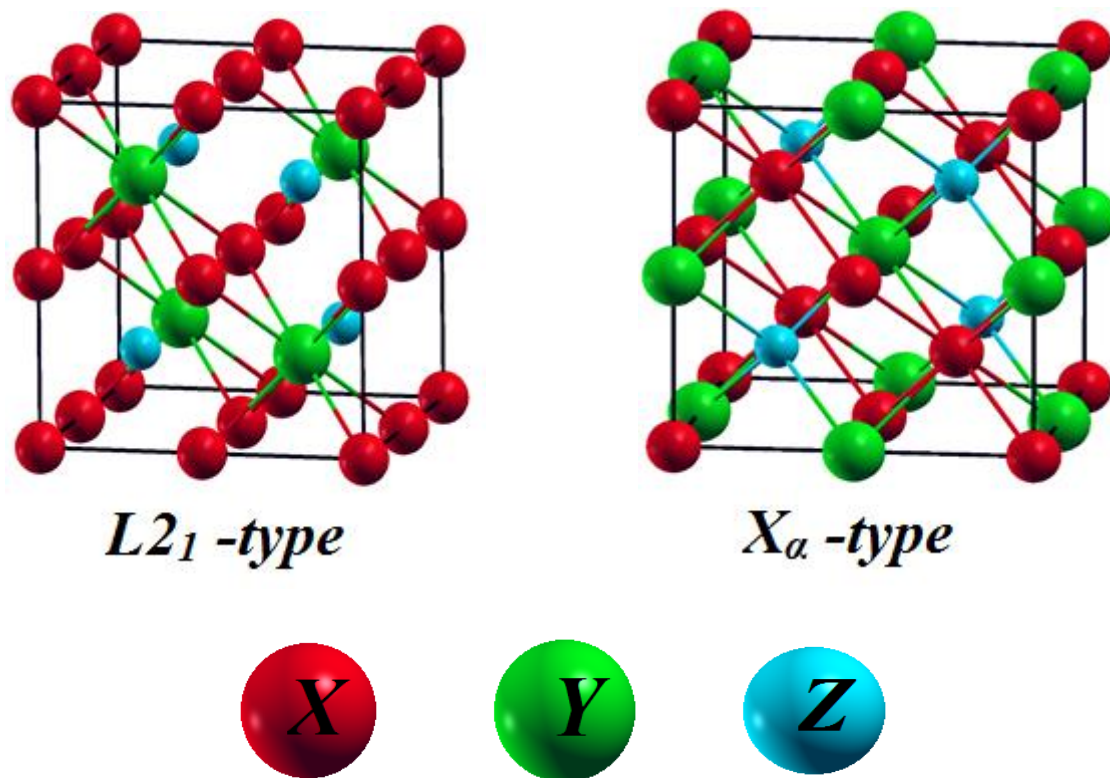


Figure II.1: Cubic crystal structure of X_2YZ full-Heusler alloys in $L2_1$ -type and X_a -type phases[3].

2-Results and discussion

This section contains the results and their discussions during the studies carried out on the structural, electronic and magnetic properties of **Sc₂-based** Full Heusler alloys

Sc₂ZrX (X = P, As and Ge).

2-1 Computational details

The results obtained in this work were carried out using the FP-LAPW method [9–14] incorporated in the Wien2K code [15]. Exchange–correlation interactions were treated using the Perdew-Burke-Ernzerhof version of the generalized gradient approximation (GGA-PBE) [16] for estimating the equilibrium structural and magnetic parameters, whereas the Tran-Blaha modified Becke Johnson approximation (TB-mBJ) [17] was used to calculate the electronic properties of the title compounds. Based on the Muffin-Tin approximation [18], the space is divided into two regions: inside the muffin-tin spheres (MT) and the interstitial region between

them. The radii of the Muffin-tin spheres of each atom were: 2.3 , 2.4 , 2.1 , 2.35 , and 2.35 Bohr for the **Sc**, **Zr**, **P**, **As** and **Ge** atoms respectively.

We indicate that the criterion and the condition of convergence of the total energy in all the calculations carried out, is equal to 10^{-4} Ry and we take the value -6 eV as energy to separate the valence states from the core states. The electronic configuration of the atoms that form the compounds **Sc₂ZrP**, **Sc₂ZrAs** and **Sc₂ZrGe** is given:

Sc: [Ar] 3d¹ 4s²

Zr: [Kr] 4d² 5s²

P : [Ne] 3s² 3p³

As: [Ar] 3d¹⁰ 4s² 4p³

Ge: [Ar] 3d¹⁰ 4s² 4p²

2-2 Convergence tests

The convergence of the calculations is well controlled by the parameter $R_{MT} \times K_{max}$ which represents the product between the minimum radius of the atomic spheres R_{MT} in the mesh unit and the magnitude of the largest vector in the plane wave expansion denoted K_{max} . The optimal value of the cutoff parameter $R_{MT}.K_{max}$ was chosen by following these steps:

Firstly; we calculate the total energy of the crystal cell for different values of $R_{MT}.K_{max}$ (between 4 and 9.5), then we traced the curve of the total energy versus $R_{MT}.k_{max}$ values as shown in Figure II.2. Through this figures, we notice that the total energy of the three compounds decreases rapidly with the increase of $R_{MT}.K_{max}$ where the total energy converges towards its minimum value from value $R_{MT}.K_{max}=8.5$.

In the same way, we tested the convergence of the optimal number of K_{points} for points-range confined between 100 and 1500 with a step of 200. The variation of the total energy according to the number of K_{points} is presented in Figure II.3. Regarding to these curves it appears that the total energy starts to converge from a number of K-points equal to 900 and the total energy becomes almost constant.

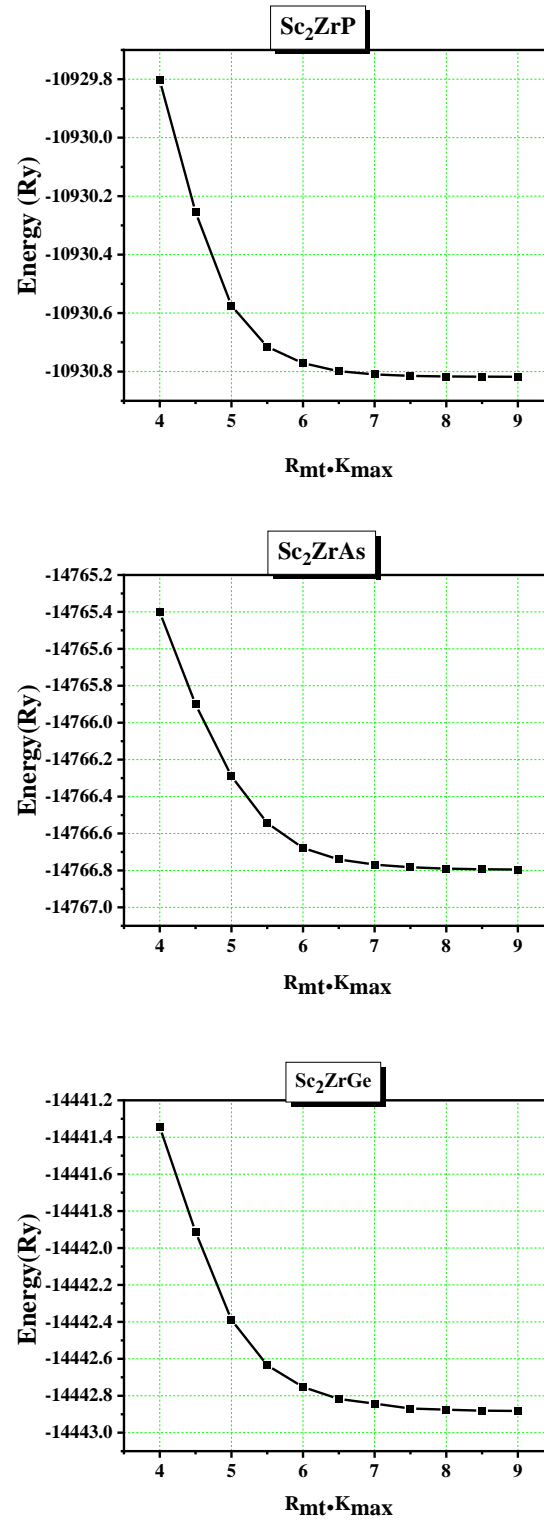


Figure II.2: Convergence test of the total energy according to $R_{MT}K_{max}$.

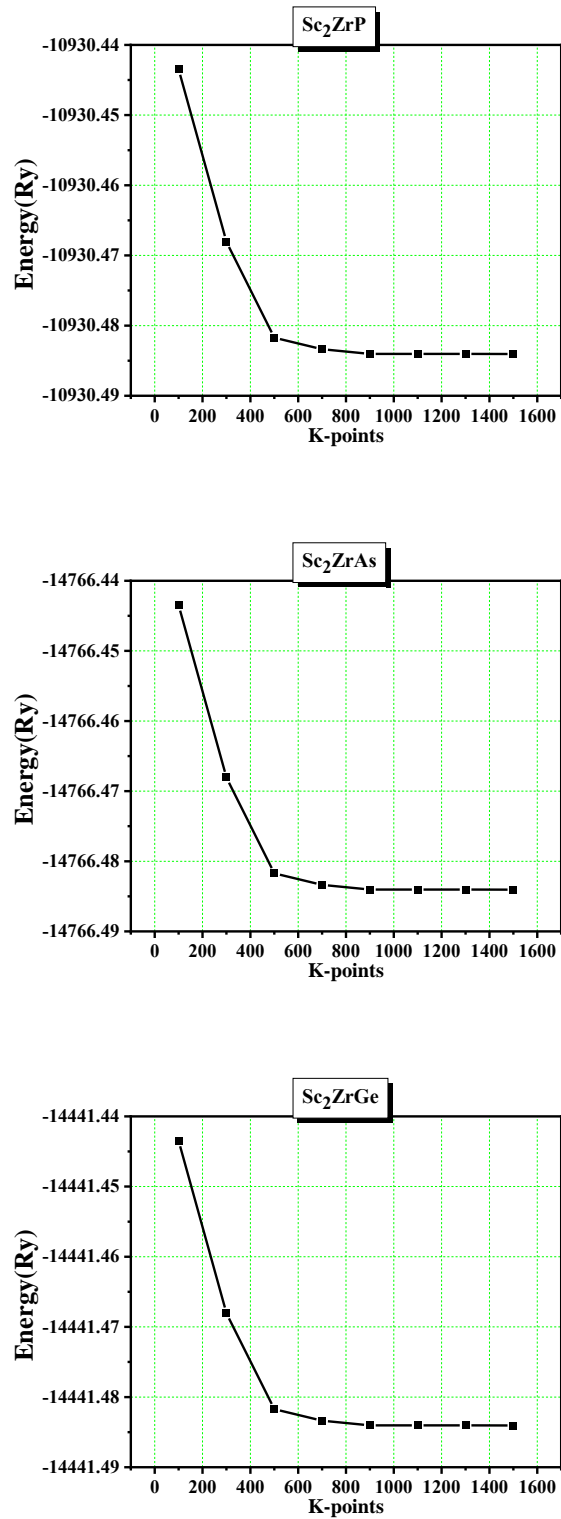


Figure II.3: Convergence test of the total energy according to k- points.

2-3 Structural properties

The following section is devoted to explore the ground state structural properties of the three compounds **Sc₂ZrX** (**X = P, As** and **Ge**) in both type structures **L2₁** and **X_α**, and thus, we estimate each of the lattice parameter (a), the bulk modulus B and its derivative B' and the cohesion energy.

The aforesaid parameters were calculated by computing the total energy of five distinct unit cell volumes for **L2₁** and **X_α** structural phases, and then we plotted the volume-energy curve by fitting the Energy-Volume curve with the Murnaghan equation [19] where this equation is written as a function of the total energy (E₀), the equilibrium volume (V₀), the bulk modulus (B) and its derivative B' as follow:

$$E(V) = E_0 + \frac{B}{B'(B'-1)} \left[V \left(\frac{V_0}{V} \right)^{B'} - V_0 \right] + \frac{B}{B'} (V - V_0)$$

From the figure II.4 we can see that, the X_α-phase (shown in black) has a lower energy than the L2₁ structural phase (shown in red) for **Sc₂ZrP** and **Sc₂ZrAs** compounds, however, the L2₁ phase is the more stable phase for the compound **Sc₂ZrGe**.

The bulk modulus B(GPa) describes the material's resistance to any deformation caused by applying external hydrostatic pressure [20], so it gives information about resistance to volume changes [21] and it can be considered as a factor used to estimate the relative stability of crystal structure, we discovered that **Sc₂ZrP** compound has the highest bulk modulus among the **Sc₂ZrAs** and **Sc₂ZrGe** compounds, implying that it has the best rigidity and aptitude to resist deformation against compression when compared to the other compounds[3,22].

However, the relatively low value of the bulk modulus ($B < 100$ GPa) suggests all the studied compounds are characterized by a relatively low resistance to volume change [23].

The cohesive energy as quantity reflects the energy required to divide a solid into its many free parts, may be used to study the cohesiveness of compounds and the physical stability of the **Sc₂ZrZ** [3]. The formula of the cohesive energy of the **Sc₂ZrZ** alloys expressed by the difference between total energy at the equilibrium point of an elementary cell and the energy of its isolated atoms **Sc**, **Zr** and **Z** like the following formula:

$$E_{cohesive} = \frac{(2 E_{atom}^{Sc} + E_{atom}^{Zr} + E_{atom}^Z) - E_{tot}^{Sc_2ZrZ}}{N_{Sc} + N_{Zr} + N_Z}$$

Where N_{Sc}, N_{Zr}, and N_Z are the number of **Sc**, **Zr** and **Z** atoms in the unit-cell of **Sc₂ZrZ** compound. According to the calculated results, we can see that **Sc₂ZrP** and **Sc₂ZrAs** Heusler

alloys have high cohesive energy in L2₁-type unlike to **Sc₂ZrGe** which was more stable structurally in X_α-type. The rest structural parameters could be found in the Table II.1

Table II.1: Structural parameters of the **Sc₂ZrX (X = P, As, Ge)** compounds calculated using GGA approximation in both **L2₁** and **X_α** structural phases.

Full Heusler Alloys	Structural properties	Our Results	
		L2 ₁	X _α
Sc ₂ ZrP	a (Å)	6.6264	6.6183
		6.7[24]	6.69[24]
	β (GPa)	91.9231	89.0796
	B' (GPa)	4.8611	4.6748
	V ₀ (a.u. ³)	490.8807	489.0798
	E ₀ (Ry)	-10930.8238	-10930.8205
	E _{Coh} (eV/atom)	4.801	4.792
Sc ₂ ZrAs	a (Å)	6.7432	6.7538
		6.86[24]	6.84[24]
	β (GPa)	86.5573	82.2059
	B' (GPa)	5.3083	4.3759
	V ₀ (a.u. ³)	517.3002	519.7395
	E ₀ (Ry)	-14766.8084	-14766.7999
	E _{Coh} (eV/atom)	4.699	4.674
Sc ₂ ZrGe	a (Å)	6.7981	6.7539
		7.11[24]	7.14[24]
	β (GPa)	80.9666	80.8376
	B' (GPa)	4.2149	3.4196
	V ₀ (a.u. ³)	530.0337	519.7672
	E ₀ (Ry)	-14442.9120	-14442.9207
	E _{Coh} (eV/atom)	4.849	4.865

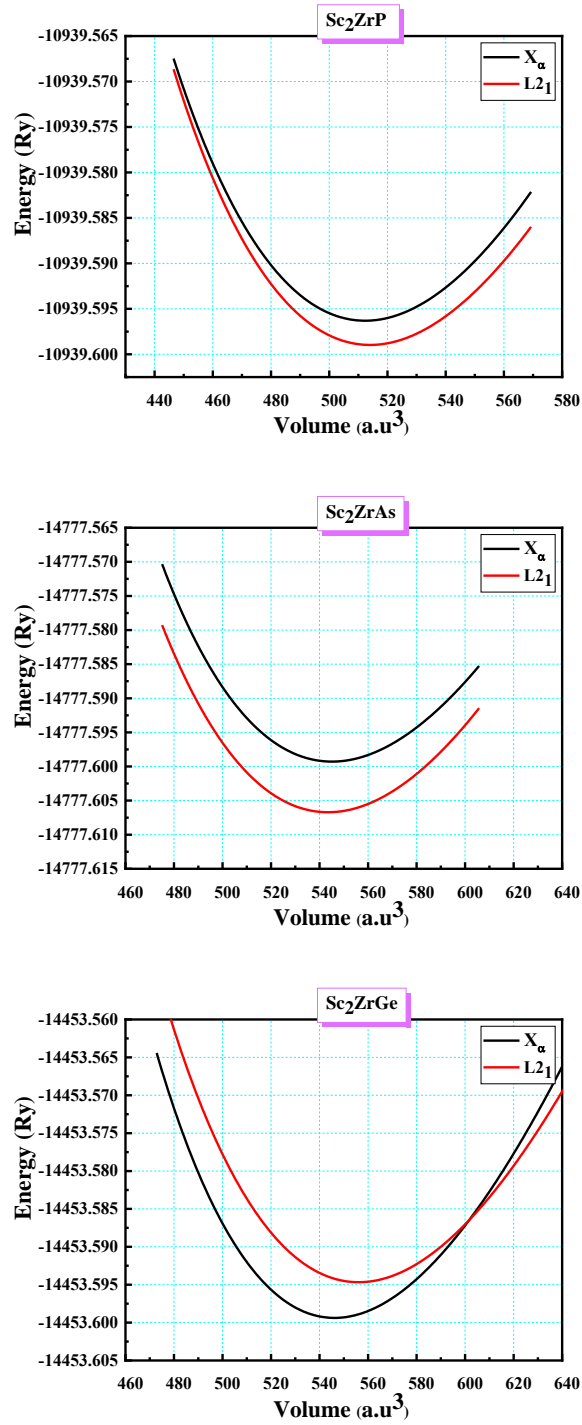


Figure II.4: Total Energy-Volume curves Sc_2ZrX ($X = \text{P}, \text{As}$ and Ge) in both type structures L_{21} and X_α calculated using GGA approximations.

2-4 Electronic properties

The study of electronic behavior is critical because it helps one to select the most appropriate electronic domain in which to employ a material. To do this, we investigated the compound's energy bands and density of state to define the orbits of the atoms that formed each band.

2-4-1 Band structure

The electrons in solid systems with a periodic structure occupy discrete energy levels, which are hybridized by the reciprocal interaction between atoms, resulting in their split into sub-levels close to each other and generating a continuous energy spectrum known as "energy band"

The band structure of **Sc₂ZrX (X = P, As, Ge)** compounds has been investigated along high symmetry directions in the most stable state in the first Brillouin zone. Figures II.5/II.6/II.7 show the band structure of **Sc₂ZrX (X = P, As, Ge)** in the most stable state determined using both GGA and mBJ approximations for the two spin directions "up" and "down". For all the studied compounds, the valence and conduction bands overlap in both directions of spins, as seen in these diagrams. As a result, in both cases of majority and minority spins, the appearance of the band structure in the ferromagnetic state exhibits metallic behavior.

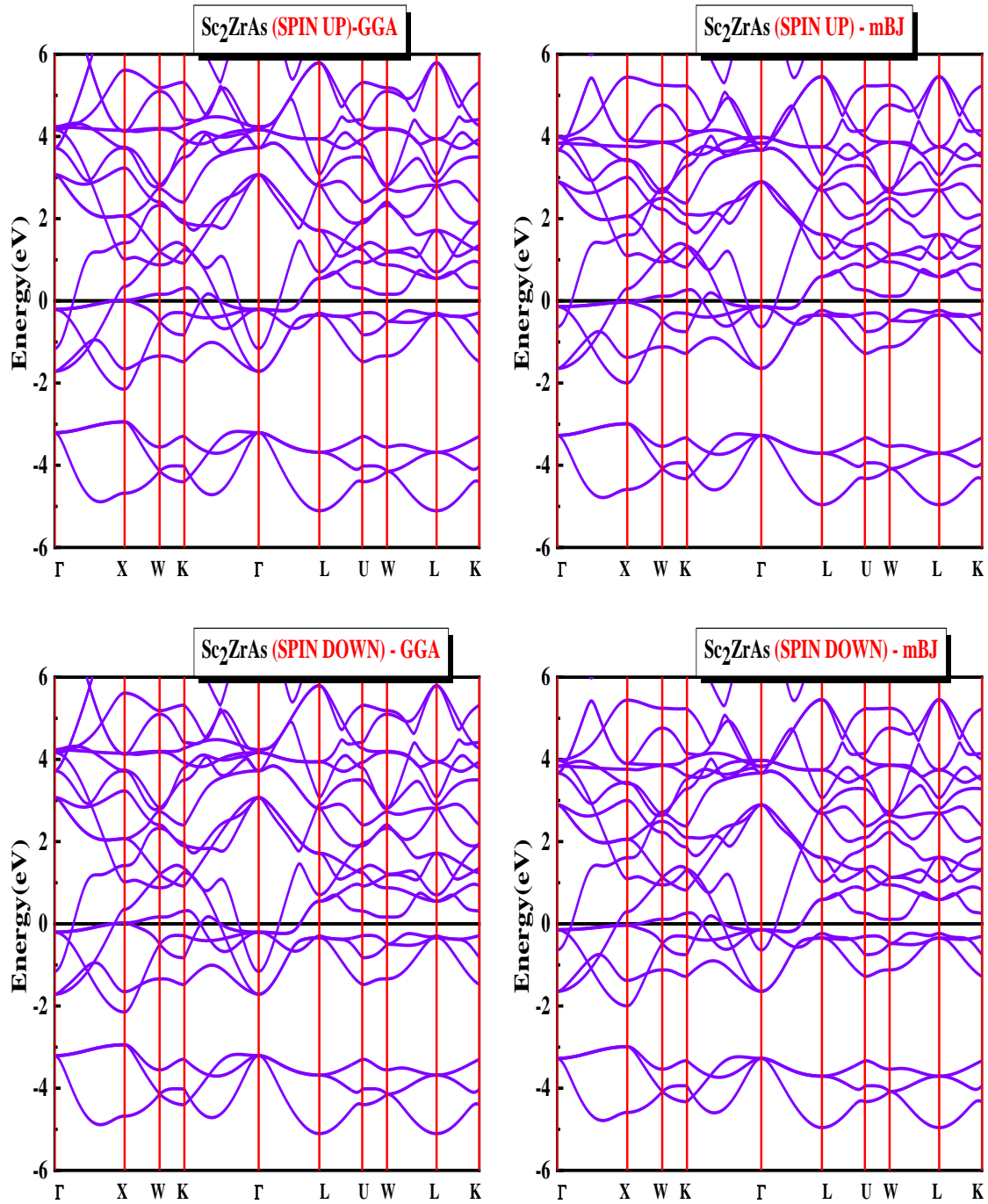


Figure II.5: Band structure of the Sc_2ZrAs compound obtained by GGA and mBJ approximations.

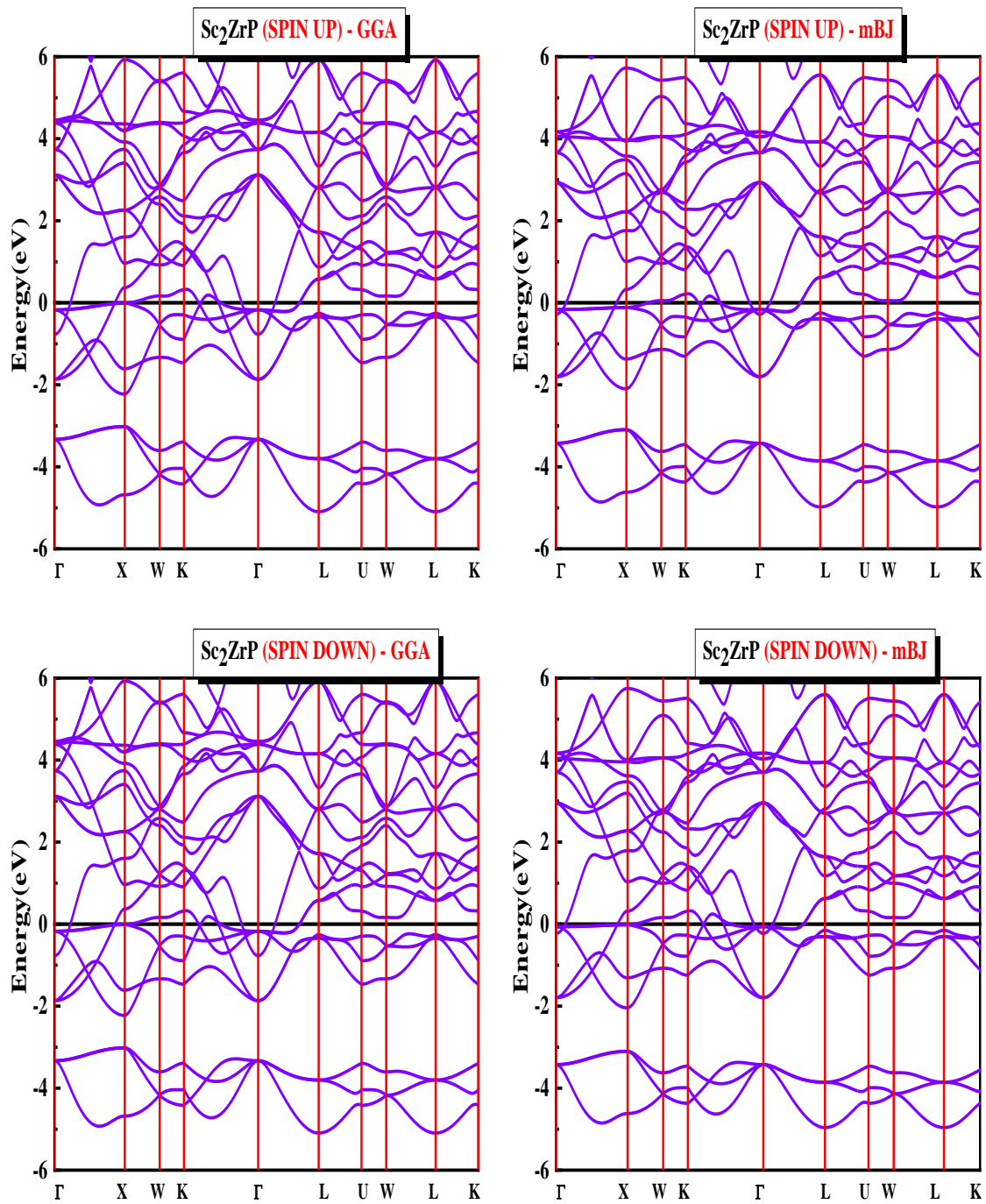


Figure II.6: The band structure of the Sc_2ZrP compound obtained by GGA and mBJ approximations.

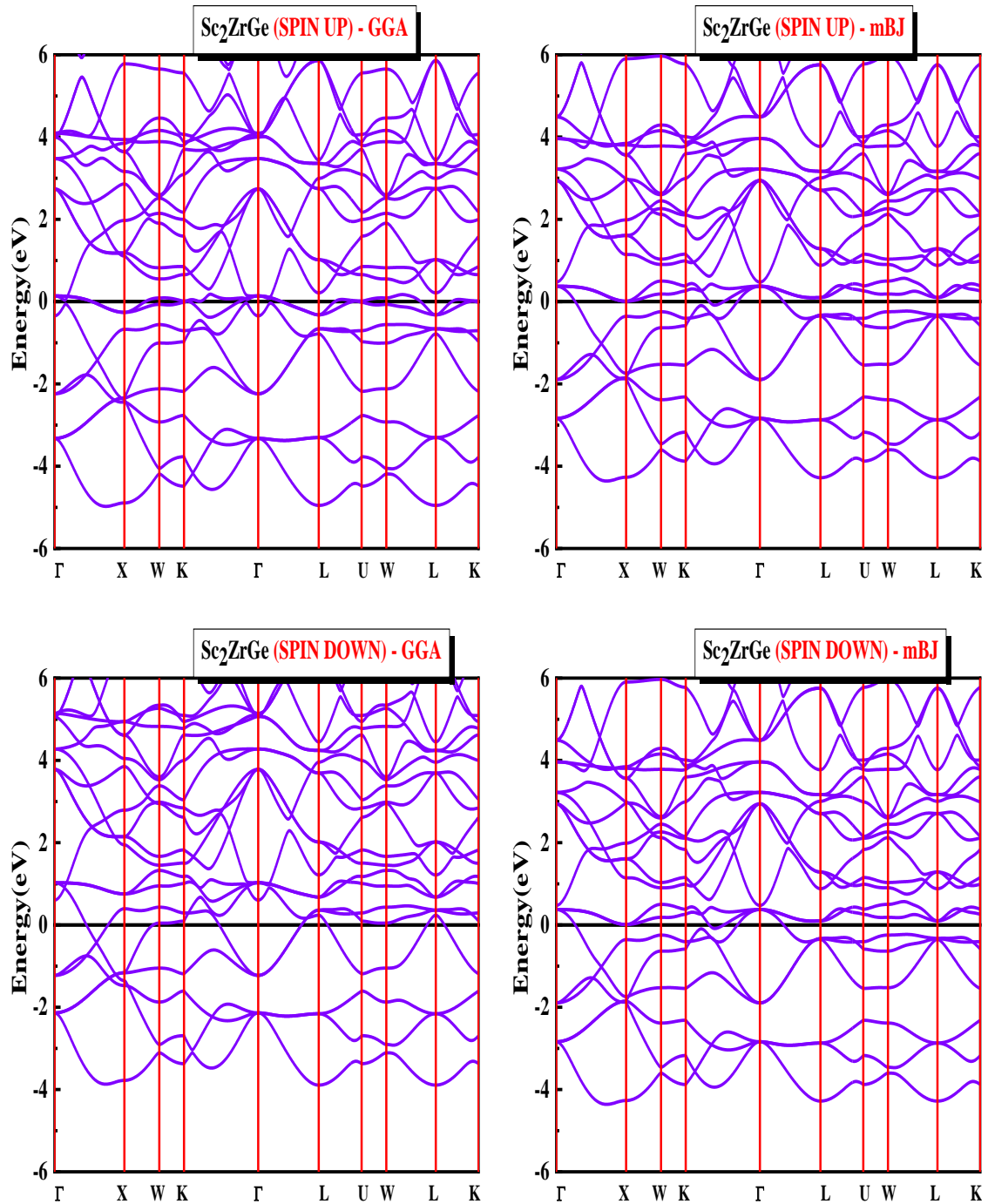


Figure II.7: The band structure of the Sc_2ZrGe compound obtained by GGA and mBJ approximations.

2-4-2 Electronic density of states

A crystal system's density of states (DOS) measures the number of electronic states with a given energy. The DOS parameter may also be used as a supplement to understand the creation of particular band structures, as well as to determine the atomic orbitals responsible for bond formation and to compute polarization.

Figures II.8/9/10/11/12/13 shows total (TDOS) and partial (PDOS) electronic state densities of the three **Sc₂ZrAs**, **Sc₂ZrP** and **Sc₂ZrGe** compounds calculated using both GGA and mBJ approximations, where the following notes can be recorded:

- We obtained almost identical curves using the previous two approximations.
- The presence of DOS values around the Fermi level for the three compounds confirms their metallic behavior.

The atomic orbitals contributions seems in Figures II.8/9 for the **Sc₂ZrAs** compound can be divided into two regions:

- 1st region located between [-5 eV, -3 eV], is mainly due to the "p" states of the Arsenic atom.
- 2nd region located between [-2 eV, +6 eV] includes strong and dominant contributions from the "d" states of both Scandium atoms and the Zirconium atom.

As for the **Sc₂ZrP** compound, according to figures II.10/11 we can divide the curves into two regions as well:

- 1st region located between [-5 eV, -3 eV], formed by the "p" states of the Phosphorus atom.
- 2nd region located between [-2 eV, +6 eV] includes strong contributions from the "d" states of the Zirconium atom and both Scandium atoms, and weak contributions from the "p" states of the Phosphorus atom.

Also, we can see from figures II.12/13, the contributions of atomic orbitals for the **Sc₂ZrGe** compound where the energetic space can be divided into three regions:

- 1st region located between [-4 eV, -2 eV], is due to the "d" states of the Zirconium atom and a weak contributions from the "p" states of the Germanium atom and the "d" states of the Scandium atoms.
- 2nd region located between [-2 eV, 0 eV] shows significant contributions from the "d" states of the Zirconium atom and a weak contributions from both Scandium atoms.
- 3rd region: the range [0 eV, +6 eV] comes from the dominant contributions of the "d" states of the Sc (1), Sc (2) and Zr atoms.

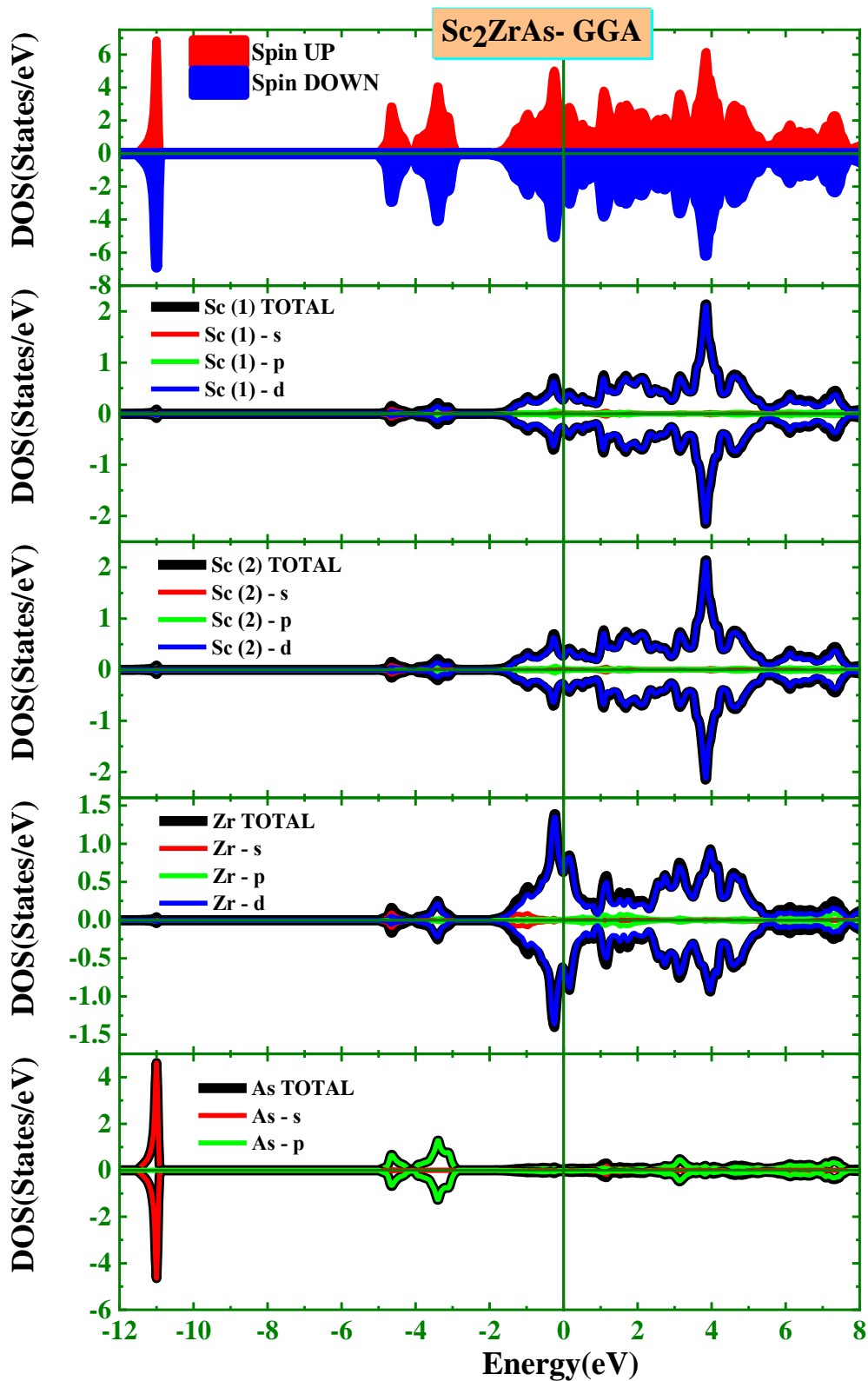


Figure II. 8: Total (TDOS) and partial (PDOS) density of states of the Sc_2ZrAs compound calculated with GGA approximation.

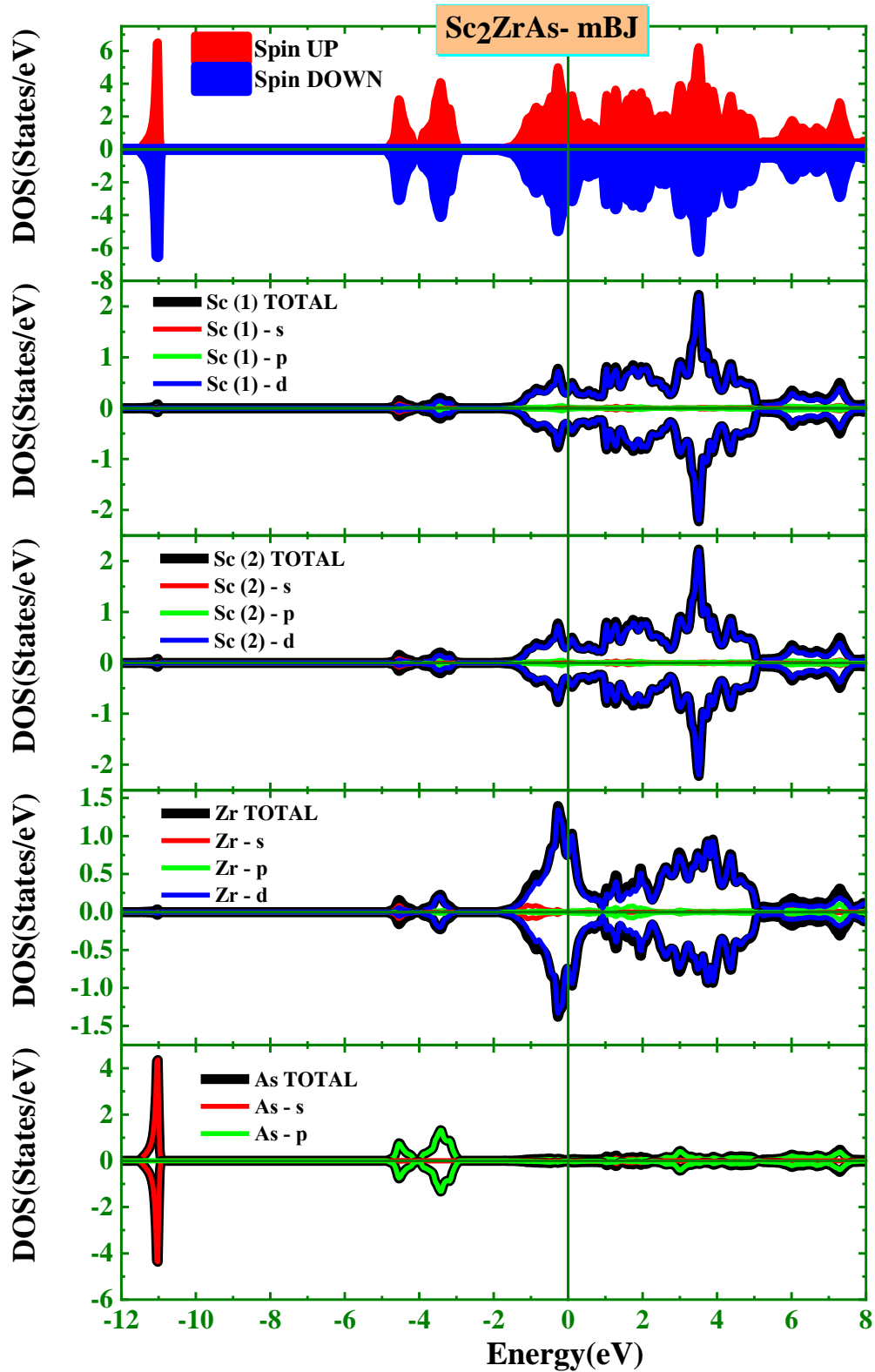


Figure II. 9: Total (TDOS) and partial (PDOS) density of states of the Sc_2ZrAs compound calculated with mBJ approximation.

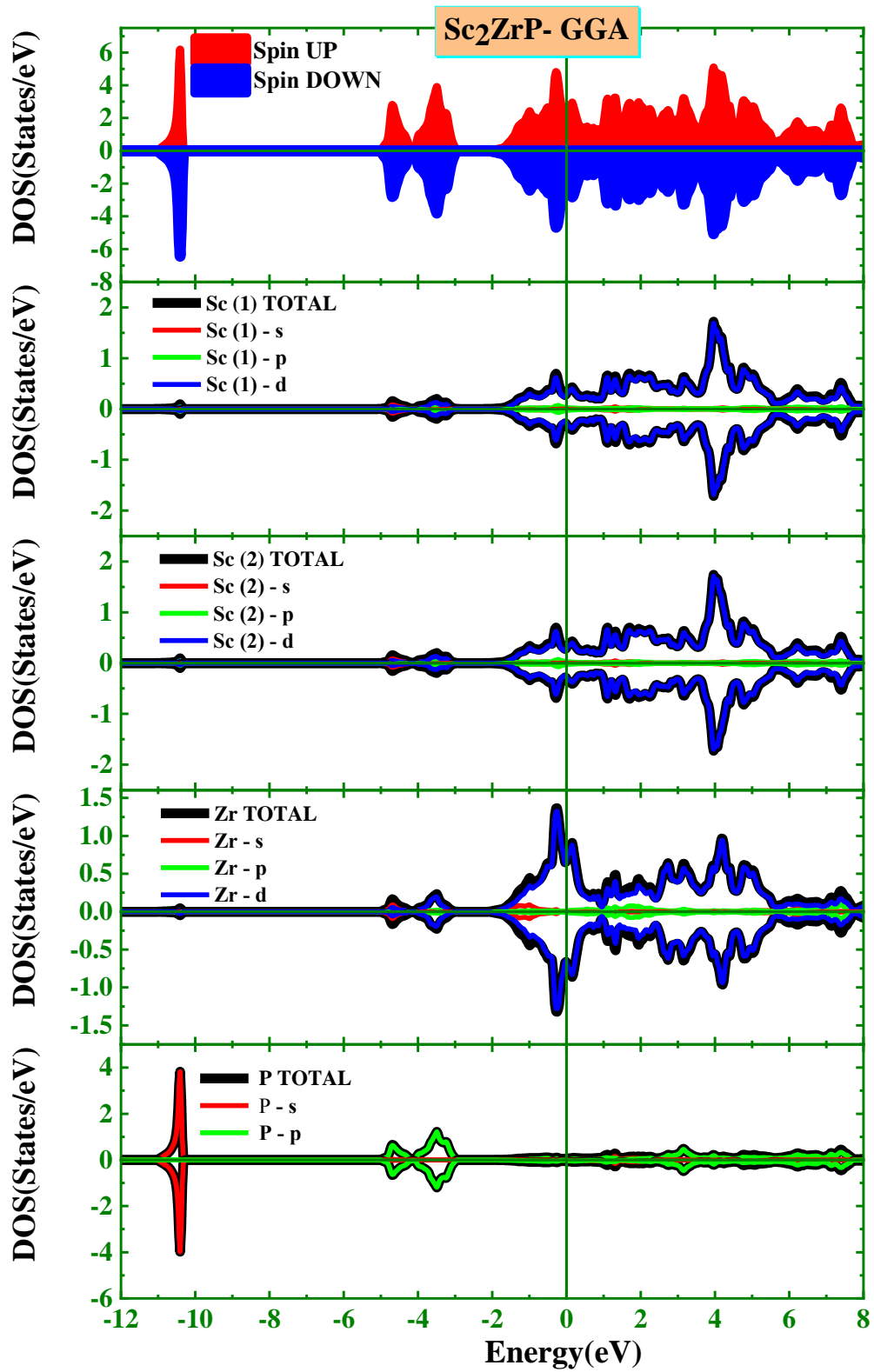


Figure II. 10: Total (TDOS) and partial (PDOS) density of states of the Sc_2ZrP compound calculated with GGA approximation.

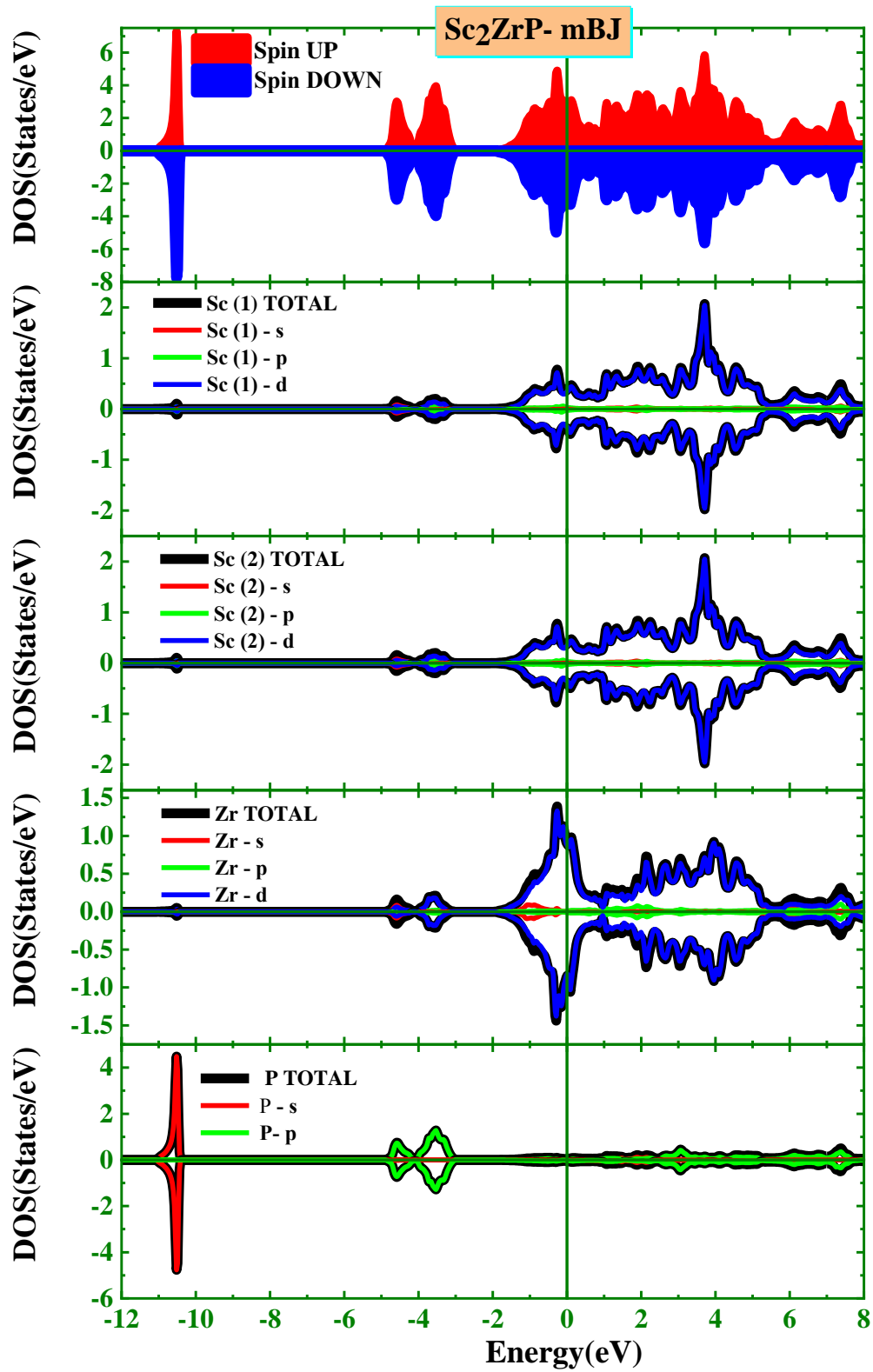


Figure II. 11: Total (TDOS) and partial (PDOS) density of states of the Sc_2ZrP compound calculated with mBJ approximation.

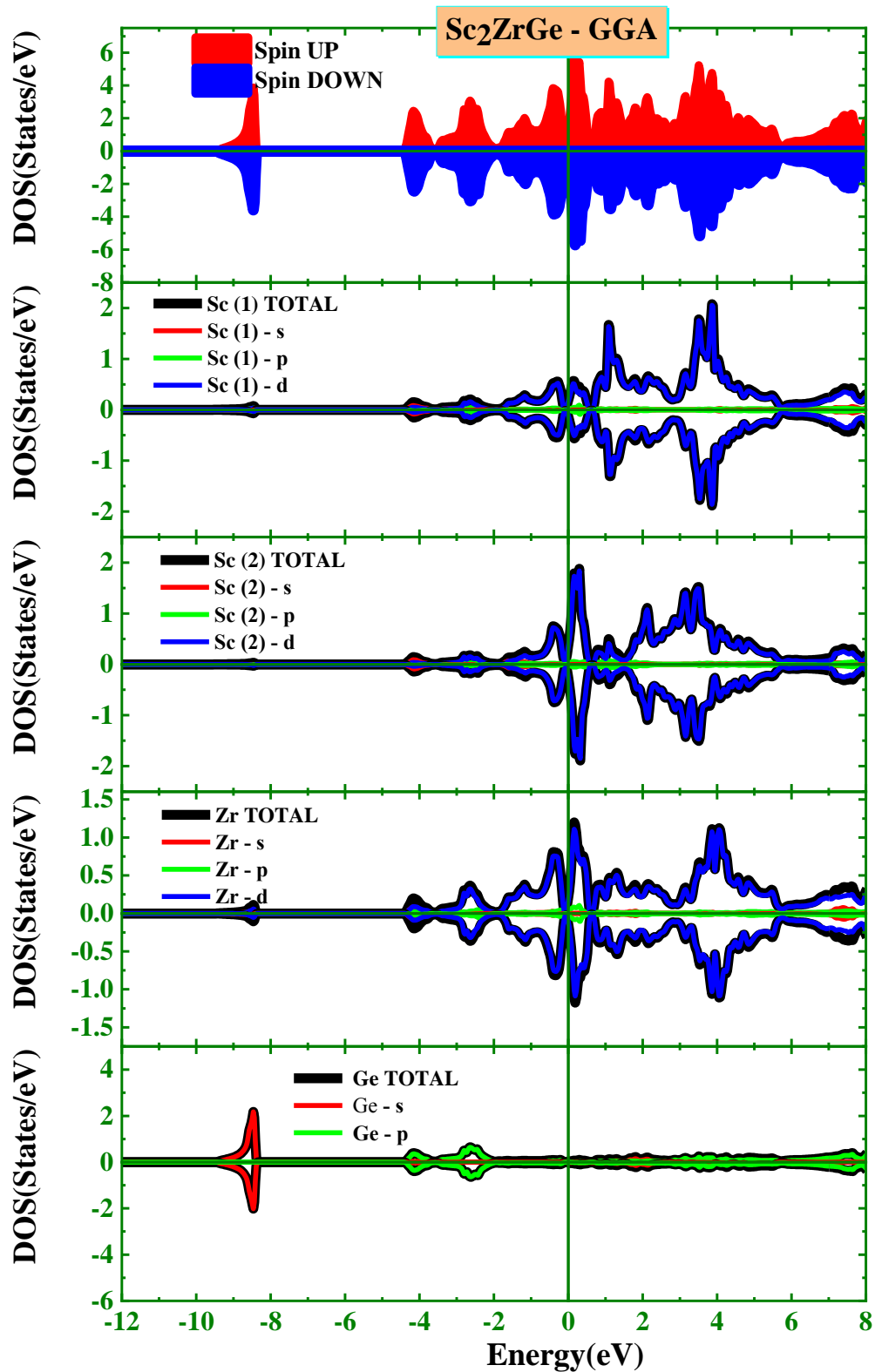


Figure II. 12: Total (TDOS) and partial (PDOS) density of states of the Sc_2ZrGe compound calculated with GGA approximation.

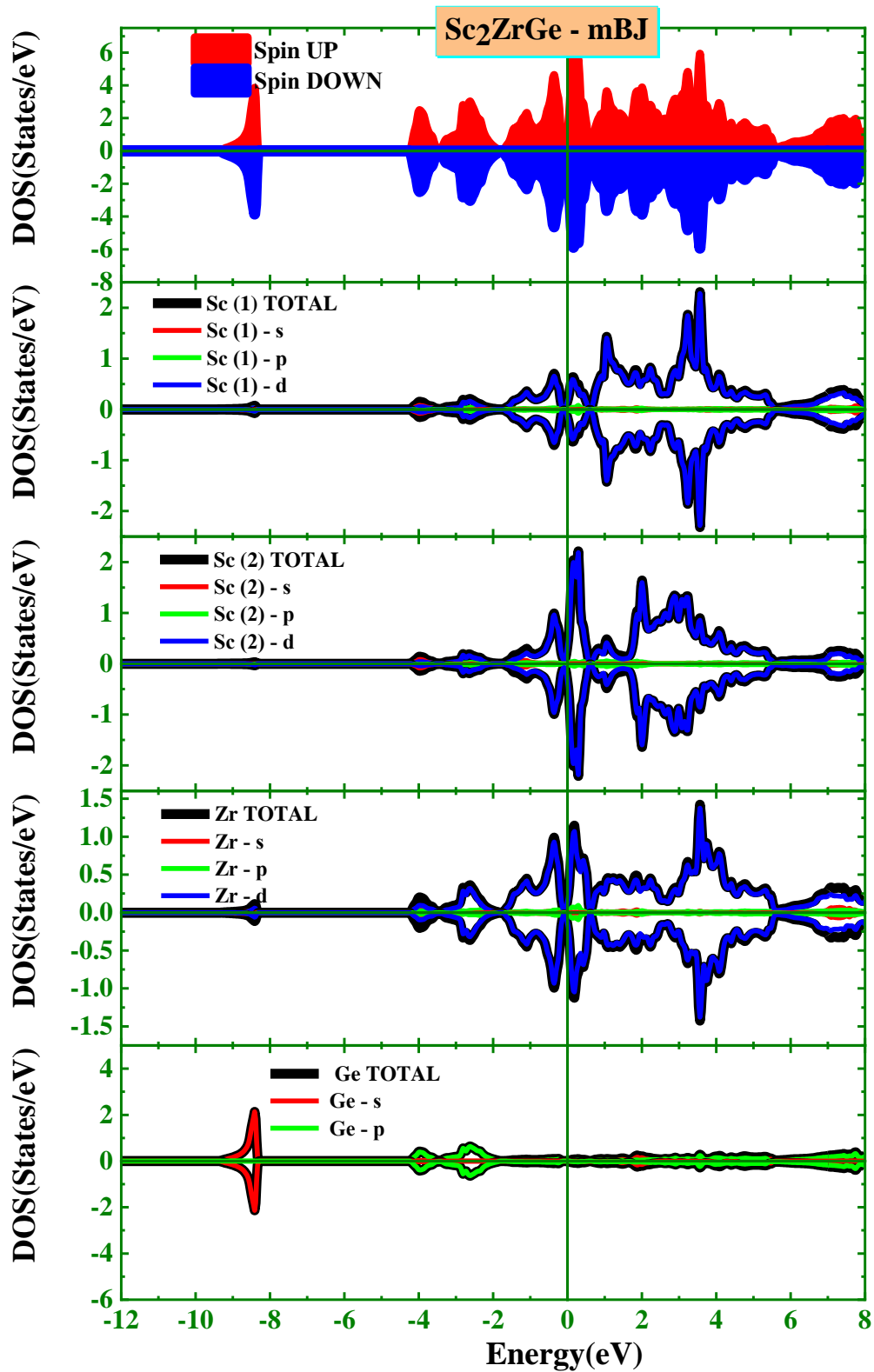


Figure II. 13: Total (TDOS) and partial (PDOS) density of states of the Sc_2ZrGe compound calculated with mBJ approximation.

2-5 Magnetic properties

We investigated the magnetic characteristics of these compounds, but first, we shall review the background of magnetism in materials, on three levels.

2-5-1 Origin of magnetism in materials

2-5-1-a Electronic level

The movement of charged particles produces a magnetic field, and as the electron is a charged particle that moves around itself and around the nucleus, these two motions produce two magnetic moments [19-24]:

- ✓ Spin magnetic moment: $\vec{\mu}_s = -g \frac{\mu_B}{\hbar} \vec{S}$ where g is the Landé parameter and \hbar the Planck constant.
- ✓ Orbital magnetic moment $\vec{\mu}_{sl} = \frac{\mu_B}{\hbar} \vec{l}$ where μ_B is the Bohr magneton.

The origin of magnetism

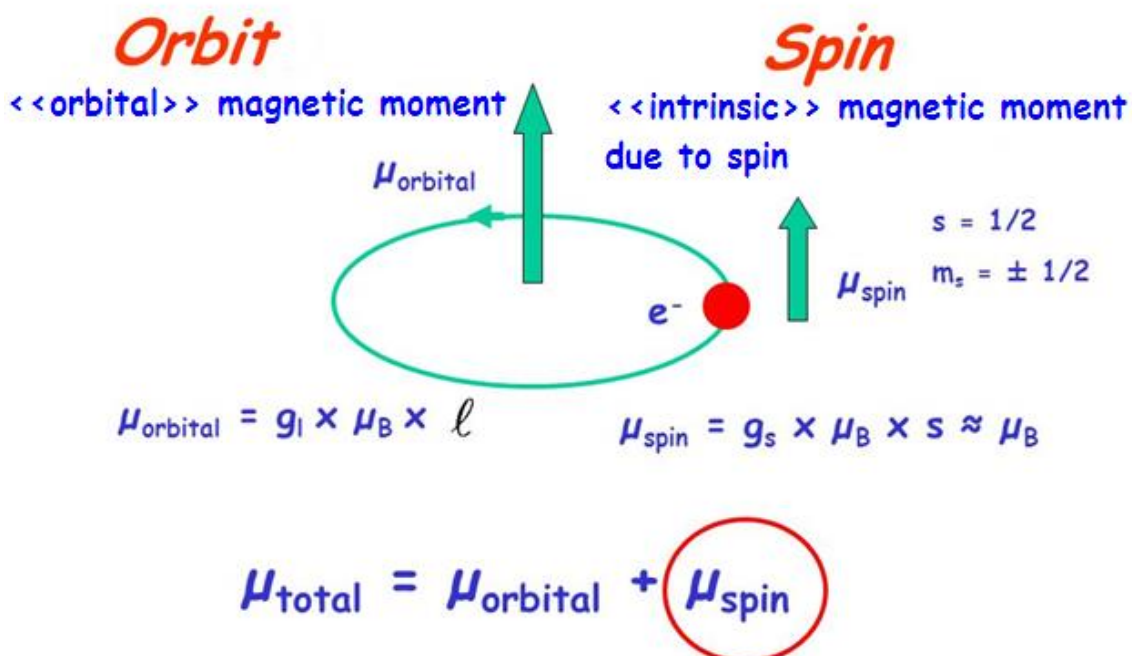


Figure II.14: Origin of magnetism at the electronic level.

2-5-1-b Atomic level

The magnetism of the atom is related to the electrons distribution in the outermost shell; if all of the electrons in its outer shell are placed in pairs, the total of their magnetic moments is zero, and the atom is non-magnetic, and vice versa.[3,22,25–29]:

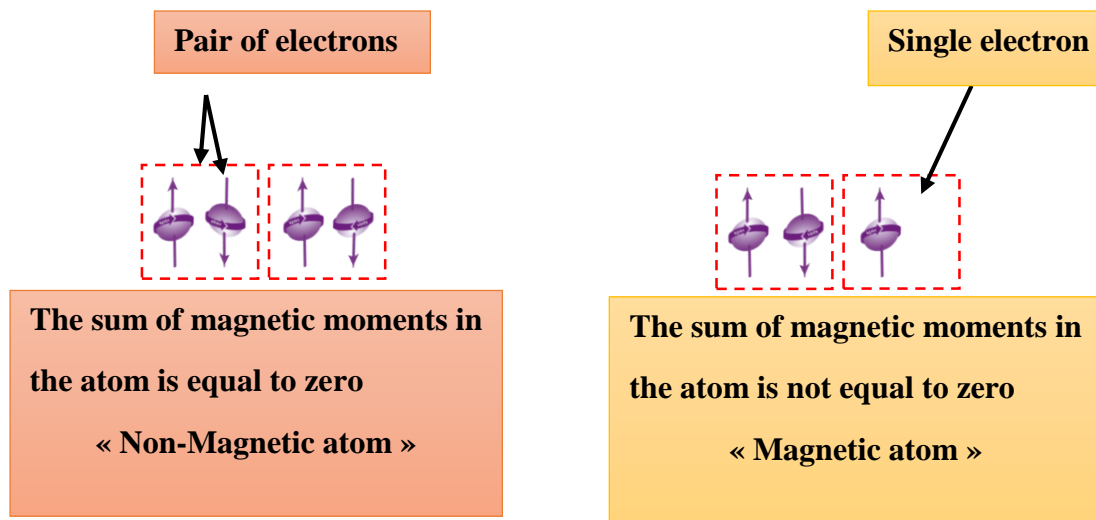


Figure II.15: Origin of magnetism at the atomic level.

2-5-1-c Material level

Magnetic potential created between atoms are quantum exchange interactions which are related to atoms magnetic moments, the distance between them, and the external magnetic field to which they are subjected. These interactions were modelled using the Heisenberg Hamiltonians given by:

$$H_{\text{mag}} = \sum_{ij} J_{ij} \vec{S}_i \cdot \vec{S}_j + \sum_i g_i \mu_B \vec{h} \cdot \vec{S}_i$$

Where μ_B is the Bohr magneton, g_i is the magnetic ratio, \vec{S}_i is the spin operator, \vec{h} is the external magnetic field, and J_{ij} is the exchange coupling constant (depends on the distance between the two atoms) [28,29]. The different types of the magnetic moments in atoms with the exchange interaction is shown in the figure II.16.

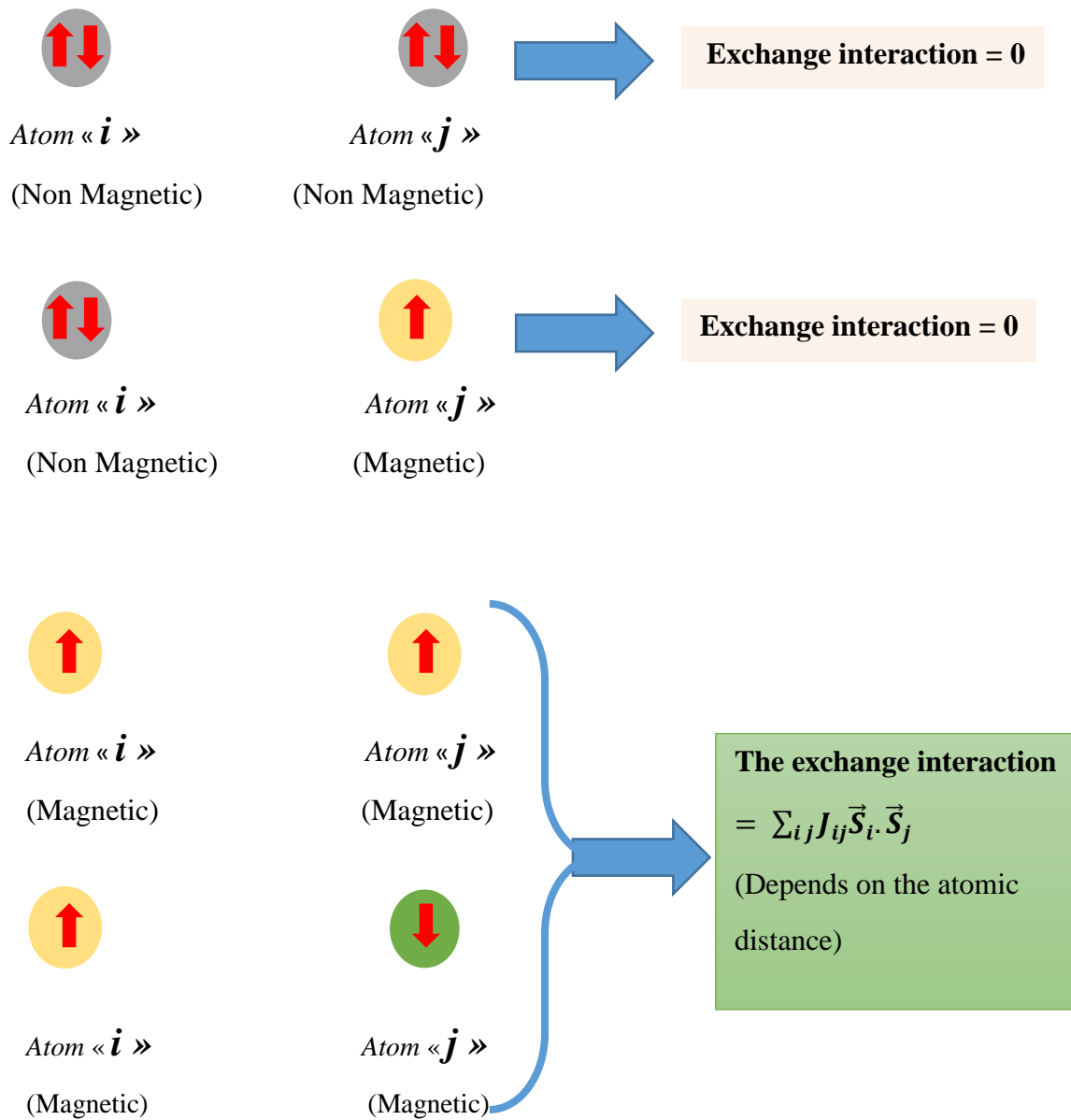
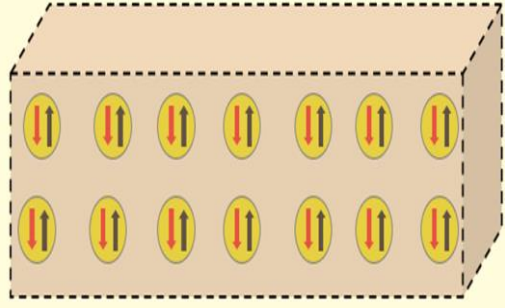
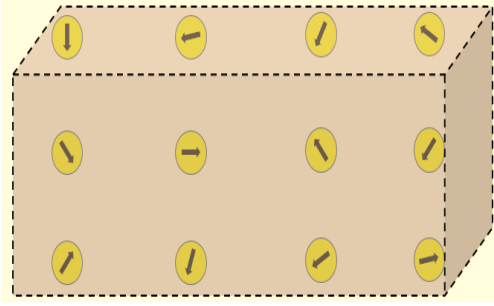
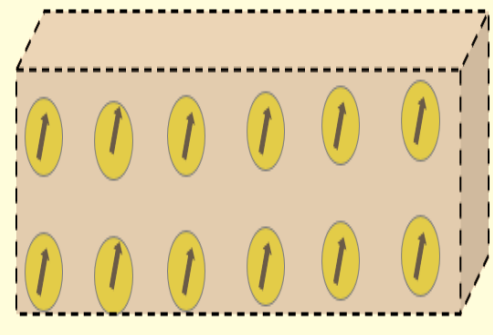


Figure II.16 : Different cases of the exchange interaction between atoms [28,29].

2-5-2 Basic types of magnetization

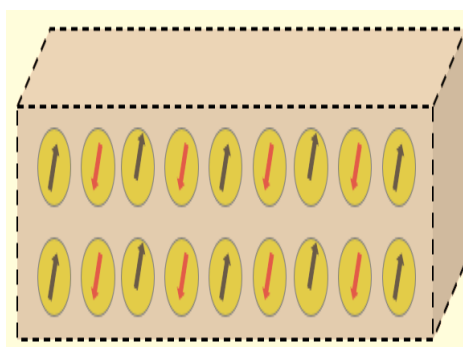
In materials, there are five types of magnetism (as seen in Table II.2 below) based on the type of the atoms that make up the material and their magnetic moments alignment [28,29].

Table II.2: Types of magnetization.

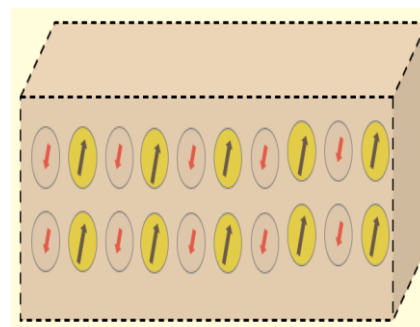
<p>a- Diamagnetism</p> <p>The diamagnetic material [3,22,25–27,30] is made up of non-magnetic atoms because all of its electrons are paired, which means that the total magnetic moment of the atoms is zero.</p>	
<p>b- Paramagnetism</p> <p>The atoms of the paramagnetic material [3,22,25–27,30] have unpaired electrons, and therefore these atoms have magnetic moments with no exchange interaction between them due to the large distance between them. Thus its magnetic moments are randomly directed so that the sum of the material's total torque is zero.</p>	
<p>c- Ferromagnetism</p> <p>The atoms of the ferromagnetic material [3,22,25–27,30] composed of unpaired electrons, the exchange interaction occurs between them due to the small distance between them, so the exchange integral J_{ij} is negative, so the electrons align in parallel.</p>	

d- Antiferromagnetism

The atoms of the antiferromagnetic material [3,22,25–27,30] composed of unpaired electrons, the exchange interaction occurs between them due to the small distance, which is small enough, that the exchange coupling constant J_{ij} is positive, so the electrons align with each other antiparallel, then the atoms arrange themselves so that two neighboring atoms can have opposite magnetic moments and consequently the moment of the material is equal to zero

**e- Ferrimagnetism**

It is a state similar to the antiferromagnetic case, except that the magnetic moments which are arranged antiparallel are not equal, and therefore, the material has a magnetic moment which is not equal to zero. [3,22,25–27,30].

**2-5-3 Magnetic properties of the Sc_2ZrX ($\text{X} = \text{P}, \text{As}, \text{Ge}$) compounds**

To classify the studied compounds (Sc_2ZrX ($\text{X} = \text{P}, \text{As}, \text{Ge}$)) according to their magnetic state, the total and partial magnetic moments of all compounds were evaluated in their most stable state (without being exposed to any external pressure or temperature impact) and recorded in Table II.3.

Studying the values of the total and partial magnetic moments of the three compounds tested in their most stable form reveals that these compounds are non-magnetic since the total moment of the crystalline cell is zero, and the partial magnetic moments of all atoms are nearly non-existent.

Table II.3: Total and partial magnetic moment of Sc_2ZrX ($X = \text{P, As, Ge}$).

<i>Compounds</i>	Magnetic moments	Results	
		GGA	mBJ
<i>Sc₂ZrP</i>	RI	-0.00289	0.06798
	Sc1	-0.00067	0.01854
	Sc2	-0.00066	0.01848
	Zr	-0.00308	0.11008
	P	0.00036	-0.00405
	Total	-0.00696	0.21104
<i>Sc₂ZrAs</i>	RI	-0.00625	-0.00250
	Sc1	-0.00151	-0.00069
	Sc2	-0.00148	-0.00069
	Zr	-0.00751	-0.00398
	As	0.00043	0.00006
	Total	-0.01633	-0.00779
<i>Sc₂ZrGe</i>	RI	-0.04699	0.00000
	Sc1	-0.01384	0.00000
	Sc2	-0.02137	0.00000
	Zr	-0.02962	-0.00000
	Ge	0.00079	-0.00000
	Total	-0.11104	0.00000

3-References

- [1] H. Kurt, J.M.D. Coey, Heusler Alloys: Properties, Growth, Applications, (2016).
- [2] A. Telfah, S.S. Essaoud, H. Baaziz, Z. Charifi, A.M. Alsaad, M.J.A. Ahmad, R. Hergenröder, R. Sabirianov, DFT Investigation of Physical Properties of KCrZ (Z=S, Se, Te) Half-Heusler alloys. , Phys. Status Solidi B. n/a (n.d).
<https://doi.org/10.1002/pssb.202100039>.
- [3] S.S. Essaoud, A.S. Jbara, First-principles calculation of magnetic, structural, dynamic, electronic, elastic, thermodynamic and thermoelectric properties of Co₂ZrZ (Z= Al, Si) Heusler alloys, J. Magn. Magn. Mater. (2021) 167984.
- [4] H. Alqurashi, R. Haleoot, B. Hamad, First-principles investigations of Zr-based quaternary Heusler alloys for spintronic and thermoelectric applications, Comput. Mater. Sci. 210 (2022) 111477.
- [5] X.-P. Wei, X. Zhang, J. Shen, W.-L. Chang, X. Tao, Gilbert damping, electronic and magnetic properties for quaternary Heusler alloys CrYCoZ: First-principles and Monte Carlo studies, Comput. Mater. Sci. 210 (2022) 111453.
- [6] K. Berarma, S. Sâad Essaoud, A.A. Mousa, S.M. Al Azar, A.Y. Al-Reyahi, Opto-electronic, thermodynamic and charge carriers transport properties of Ta₂FeNiSn₂ and Nb₂FeNiSn₂ double half-Heusler alloys, Semicond. Sci. Technol. (2022).
<https://doi.org/10.1088/1361-6641/ac612b>.
- [7] S. Anand, M. Wood, Y. Xia, C. Wolverton, G.J. Snyder, Double half-heuslers, Joule. 3 (2019) 1226–1238.
- [8] I. Jum'h, H. Baaziz, Z. Charifi, A. Telfah, Electronic and Magnetic Structure and Elastic and Thermal Properties of Mn 2-Based Full Heusler Alloys, J. Supercond. Nov. Magn. 32 (2019) 3915–3926.
- [9] J.C. Slater, Damped electron waves in crystals, Phys. Rev. 51 (1937) 840.
- [10] D.D. Koelling, G.O. Arbman, Use of energy derivative of the radial solution in an augmented plane wave method: application to copper, J. Phys. F Met. Phys. 5 (1975) 2041.
- [11] O.K. Andersen, Linear methods in band theory, Phys. Rev. B. 12 (1975) 3060.
- [12] D.R. Hamann, Semiconductor charge densities with hard-core and soft-core pseudopotentials, Phys. Rev. Lett. 42 (1979) 662.
- [13] D. Singh, H. Krakauer, H-point phonon in molybdenum: Superlinearized augmented-plane-wave calculations, Phys. Rev. B. 43 (1991) 1441.
-

-
- [14] E. Sjöstedt, L. Nordström, D.J. Singh, An alternative way of linearizing the augmented plane-wave method, *Solid State Commun.* 114 (2000) 15–20.
- [15] P. Blaha, K. Schwarz, G. Madsen, D. Kvasnicka, J. Luitz, *Wien2k*, (2001).
- [16] J.P. Perdew, K. Burke, M. Ernzerhof, Generalized gradient approximation made simple, *Phys. Rev. Lett.* 77 (1996) 3865.
- [17] A.D. Becke, E.R. Johnson, A simple effective potential for exchange, *American Institute of Physics*, 2006.
- [18] O.K. Andersen, T. Saha-Dasgupta, Muffin-tin orbitals of arbitrary order, *Phys. Rev. B.* 62 (2000) R16219.
- [19] F.D. Murnaghan, The compressibility of media under extreme pressures, *Proc. Natl. Acad. Sci. U. S. A.* 30 (1944) 244.
- [20] M.E. Ketfi, H. Bennacer, S.S. Essaoud, M.I. Ziane, A. Boukortt, Computational evaluation of optoelectronic, thermodynamic and electron transport properties of CuYZ₂ (Z= S, Se and Te) chalcogenides semiconductors, *Mater. Chem. Phys.* (2021) 125553.
- [21] A. Benamer, Y. Medkour, S.S. Essaoud, S. Chaddadi, A. Roumili, Ab-initio study of the structural, electronic, elastic and thermodynamic properties of Sc₃XB (X= Sn, Al, Hf), *Solid State Commun.* 331 (2021) 114305.
- [22] S. Saad Essaoud, *Les composés à base de manganèse: investigation théorique des propriétés structurales électroniques et magnétiques*, 2020.
<https://doi.org/10.13140/RG.2.2.30742.68169>.
- [23] S. Sâad Essaoud, A. Bouhemadou, S. Maabed, S. Bin-Omran, R. Khenata, Pressure dependence of the electronic, optical, thermoelectric, thermodynamic properties of CsVO₃: first-principles study, *Philos. Mag.* (2022) 1–25.
<https://doi.org/10.1080/14786435.2022.2057611>.
- [24] Y. Han, Z. Chen, M. Kuang, Z. Liu, X. Wang, X. Wang, 171 Scandium-based full Heusler compounds: A comprehensive study of competition between XA and L21 atomic ordering, *Results Phys.* 12 (2019) 435–446.
- [25] S.S. Essaoud, Z. Charifi, H. Baaziz, G. Uğur, Ş. Uğur, Electronic structure and magnetic properties of manganese-based MnAs_{1-x}P_x ternary alloys, *J. Magn. Magn. Mater.* 469 (2019) 329–341.
- [26] O. Volnianska, P. Boguslawski, Magnetism of solids resulting from spin polarization of p orbitals, *J. Phys. Condens. Matter.* 22 (2010) 073202. <https://doi.org/10.1088/0953-8984/22/7/073202>.
-

- [27] J.M.D. Coey, ed., Magnetism of localized electrons on the atom, in: Magn. Magn. Mater., Cambridge University Press, Cambridge, 2010: pp. 97–127.
<https://doi.org/10.1017/CBO9780511845000.005>.
- [28] H. Amina, Etude théorique des propriétés structurales, électroniques et magnétiques du composé Co₂AlB₂., PhD Thesis, UNIVERSITE MOHAMED BOUDIAF-M'SILA, 2021.
- [29] للمركب CsVO₃ ل. مروة, دراسة الخواص الكهرو حرارية والترموديناميكية, Master Thesis, UNIVERSITE MOHAMED BOUDIAF-M'SILA, 2021.
- [30] I. Jum'h, H. Baaziz, Z. Charifi, A. Telfah, Electronic and Magnetic Structure and Elastic and Thermal Properties of Mn 2-Based Full Heusler Alloys, J. Supercond. Nov. Magn. (n.d.) 1–12.

Conclusion

Conclusion

This thesis included a theoretical analysis of the structural, electronic, and magnetic characteristics of three compounds, **Sc₂ZrP**, **Sc₂ZrAs**, and **Sc₂ZrGe**, using the Wien2k simulation code and the density functional theory "DFT" based on the full-potential linearized augmented-plane wave (FP-LAPW) approach.

The fundamental objective of this work was realized, in which the foundations of quantum mechanics were applied to determine the appropriate field for using these compounds, as well as knowing the influence of the type of atoms on certain properties, which allows us to predict additional materials with better properties.

Through our study, we took note of the following observations:

- ✓ The three compounds crystallize in a cubic structure that has a large level of symmetry, so it is easy for us to perform the calculations in a short time.
- ✓ The methods employed to estimate the exchange-correlation potential produced results extremely close to the experimental data, indicating that the experimental and theoretical sides are in excellent accordance.
- ✓ **Sc₂ZrP** compound is more resistant to external pressure than the other two compounds after calculating the Bulk modulus and the cohesive energy.
- ✓ The three compounds have a metallic behavior, which when analyzing the electronic band structure we observed an overlap between the conduction band and the valence band.
- ✓ By studying magnetic properties we can see that these compounds are non-magnetic compounds.

ملخص

قمنا بدراسة نظرية لحساب الخواص البنيوية، الإلكترونية والمغناطيسية لثلاثة مركبات هي **Sc₂ZrP** و **Sc₂ZrAs** و **Sc₂ZrGe** في إطار نظرية دالية الكثافة (DFT) وباستعمال برنامج Wien2k المعتمد على طريقة الامواج المستوية المتزايدة خطيا (FP_LAPW) وهذا بالاعتماد على كل من تقريب التدرج المعمم (GGA) والتقريب المعدل (mBJ) لحساب كمون تبادل_ارتباط . فيما يخص الخواص البنيوية، حددنا قيم كل من ثابت الشبكة، معامل الانضغاطية وطاقة التماسك. ولفهم السلوك الإلكتروني لكل مركب قمنا بحساب وتحليل بنية عصابات الطاقة الإلكترونية وكثافة الحالة الإلكترونية الكلية (TDOS) والجزئية (PDOS). ومن جهة أخرى قمنا أيضا بدراسة العزم المغناطيسي الكلي والجزئي للذرات المكونة للمركبات الثلاثة.

Abstract

A theoretical study of structural, electronic and magnetic properties for **Sc₂ZrP**, **Sc₂ZrAs** and **Sc₂ZrGe** was done in the framework of the density functional theory (DFT) and using the Wien2k code based on the full-potential linearized augmented plane wave method (FP_LAPW). We used both generalized gradient approximation (GGA) and modified Becke-Johnson approximation (mBJ) to calculate the correlation-exchange potential. Concerning the structural properties, we determined the values of the lattice constant, the Bulk modulus and the cohesive energy. To understand the electronic behavior of each compound, we calculated and analyzed the structure of the electronic band-structure, the total density of state (TDOS) and partial density of state (PDOS). On the other hand, we also studied the partial and total magnetic moment of the atoms forming the three compounds.

Résumé

Une étude théorique a été effectuée pour calculer les propriétés structurales, électroniques et magnétiques des composés **Sc₂ZrP**, **Sc₂ZrAs** et **Sc₂ZrGe**, dans le cadre de la théorie de la fonctionnelle de la densité (DFT) et en utilisant le code Wien2k basé sur la méthode des ondes planes augmentées linéarisées (FP_LAPW). En utilisant à la fois de l'approximation de gradient généralisée (GGA) et de l'approximation de Becke-Johnson modifiée (mBJ) pour calculer le potentiel d'échange et de corrélation. Concernant les propriétés structurales, nous avons déterminé les valeurs du paramètre de la maille, le module de compressibilité et de l'énergie cohésion. Pour comprendre le comportement électronique de chaque composé, nous avons calculé et analysé la structure des bandes d'énergie électronique, la densité totale d'état électronique (TDOS) et la densité partielle d'état électronique (PDOS). D'autre part, nous avons également étudié le moment magnétique partiel et total des atomes formant les trois composés.